Manuscript prepared for Biogeosciences Discuss.
with version 2014/05/30 6.91 Copernicus papers of the LaTeX class copernicus.cls.
Date: 14 August 2014

Simulated anthropogenic CO_2 uptake and acidification of the Mediterranean Sea

J. Palmiéri[1,2], J. C. Orr[1], J.-C. Dutay[1], K. Béranger[2], A. Schneider[3], J. Beuvier[4,5], and S. Somot[5]

[1]LSCE/IPSL, Laboratoire des Sciences du Climat et de l'Environnement, CEA-CNRS-UVSQ, Gif-sur-Yvette, France
[2]ENSTA-ParisTech, Palaiseau, France
[3]GEOMAR; Helmholtz-Zentrum für Ozeanforschung Kiel, Germany
[4]Mercator Ocean, Ramonville Saint-Agne, France
[5]CNRM/Météo-France, Toulouse, France

Correspondence to: J. Palmiéri (julien.palmieri@lsce.ipsl.fr)

1 Response to Referee #1 (Marta Alvarez)

We are grateful for the assessment by Referee #1, whose comments are repeated below (in gray) with each one followed by our response (in black).

This work deals with a relevant topic for the Mediterranean Sea environment. This marginal sea suffers a high human pressure in different social, economical and environmental issues. The present work tries to estimate the anthropogenic CO2 uptake and storage and the directly derived pH decrease (acidification) in the water column in this practically closed system using a modelling approach. This issue is of particular interest to the referee. I agree that the work tries to address relevant questions for the oceanographic community working the MedSea but also for policy makers and it deserves publication in Biogeosciences but first it needs some MAJOR IMPROVEMENTS regarding the comments below.

We are happy that Referee #1 feels that this work should be published after some revisions.

I guess that applying your model results to one or other data base in the Mediterranean Sea is not a major issue if the cruises are recent and coherent in the CO2 data. Although I am biased, I really miss some reference to Álvarez et al. (Oc. Science 2014), this data was available in CDIAC from mid 2012 (http://cdiac.ornl.gov/oceans/Coastal/Meteor_Med_Sea.html) and it could have been used to get a better resolution of alkalinity, combining both 2001 and 2011 data sets. I am aware of other basin-scale cruises but the data is not so easily available. Although no TTD results are available for the 2011 data set, the directly measured tracer concentrations are contained in the data base.

Unfortunately, Alvarez et al. (2014) was not published before we designed our simulations, ran them, and compared them with the TTD data-based estimates. Nor does that publication provide a relationship for total alkalinity vs. salinity in the Med Sea. Our objective was not to derive a new salinity-alkalinity relationship, a noble goal but not within our remit of simulating anthropogenic CO_2 uptake. Instead, we used the published surface salinity-alkalinity relationship from Schneider et al. (2007) to derive the coefficients used for the perturbation approach in one of our 3 simulations (VAR). Results from the other 2 simulations do not depend on a variable salinity. Another reason for that was that the same salinity-alkalinity relationship was

used in the TTD method of Schneider et al. (2010), which provided internal consistency with the rest of the study. We consider that the carbonate system and hydrographic data collected on the older 2001 cruise (METEOR M51/2) was of high quality and adequate for our purposes. Regardless of these concerns, we have now read Alvarez et al. (2014) and will cite it in the revised manuscript.

1) One of my main concerns is commented in the Introduction, last paragraph in page 6464 and first paragraph in page 6465: the MedSea is warming and getting saltier at higher rates than any other ocean, ventilation of deep waters is much faster as well, in addition, it has a very peculiar CO2 chemistry (Álvarez et al., 2014). So I wonder if your model approach is somehow simplistic (I am not a modeller, so please excuse me!), does your model consider changes in salinity and temperature and how they affect the CO2 chemistry (TA for example), and even more, we know that the Revelle factor increases as pCO2 increases, making the waters less able to store CANT. I know it is complicated but the options in the model GLO-TA as in the global ocean, Med: mean TA equal to MedSEa values and VAR: salinity variations taken into account although interesting, could go a little bit further. What happens to the VAR option if including temperature & salinity increase and the feedback in the CO2 system?. Maybe using the temporal change in the buffer factors (as defined in Egleston et al. but formulated correctly in Alvarez et al 2014) could help to calculate the change in the CO2 system.

Of course, our model is a simplification, by definition. However, we do indeed account for physical changes (temperature and salinity increases) and the Med Sea's rapid ventilation of deep waters. Our physical model is driven by reanalysis data over roughly the last 50 years. Thus, we force the model with observed winds, heat fluxes, and water fluxes (evaporation minus precipitation) during that time. The modelled Med Sea also has more rapid ventilation of deep waters in our model of the Med Sea (relative to the global ocean), although it is still too weak, based on CFC-12 evaluation, as we point out in the manuscript.

For carbonate chemistry, we used the equations and constants recommended for best practices to derive our perturbation approach. With this approach our model certainly does account for the increase in the Revelle factor (reduced buffer capacity) as atmospheric CO_2

increases. There is no need for us to use the buffer factors from Egleston et al. (2010) for the model simulations. The effects of increases in temperature, salinity, and CO_2 are all included in our model. We shall try to make this clearer in the revised manuscript.

2) Section 2.2.2 Anthropogenic carbon. I am sorry but I do not get the message from here. The driver is the pCO2 atmospheric increase, δpCO$_2$ocean is calculated from the only tracer that is carried in the model δC_T (page 6470, lines 14-15) using Eq. 12 & 13 . So why do you calculate δpCO$_2$ocean?, is it needed in the model for something additional?. I do understand that δC_T is calculated as the difference between the preindustrial value and the new one in time x as a function of pCO$_2$ air in time x, TA, temperature and salinity (page 6471). And in the VAR simulation TA is calculated from Eq 11, in the other two is constant. SO I do not get why do you need δpCO$_2$ocean and the empirical Eq. 13.

We must calculate oceanic δpCO$_2$ from δC_T because we need the former to compute the air-sea flux of anthropogenic CO_2 (see equation 5) and only the latter is transported as a passive tracer in the model. That is, in our model the oceanic δpCO$_2$ is not the same as the atmospheric δpCO$_2$, unlike in equilibrium calculations that assume that the two are equal. The two must be different for there to be an air-sea flux of anthropogenic CO_2, both in the model and in the real ocean. Our equation 13 is actually the 3 equations for the coefficients that are needed to compute δpCO$_2$ from δC_T in equation 12 (for the VAR simulation). Without these relationships we could not compute the air-sea flux of anthropogenic CO_2. We did explain this in the Discussion paper, but we will try to clarify further in the revised manuscript.

3) Section 2.3 Looping.
Sorry again but I am afraid that only modellers would understand this section It could be nice to explain for lay people what means "run off-line, looping through the circulation fields...".

In the revised manuscript, we will improve this section to be more understandable to non-modelers, in particular to better explain the offline approach and the looping. Offline means that first a simulation is made with the general circulation model (circulation model only), and then those simulated circulation fields are used later to drive other simulations that

include additional passive tracers such as C_T. Offline simulations are done for computational efficiency. They allow us to read in precomputed transport fields instead of recomputing them, which is very costly. They also allow us to make sensitivity tests (e.g., our simulations GLO, MED, and VAR) that use exactly the same circulation fields each time.

4) Section 2.4 δpH.

For surface or deep waters you would need to clarify if δpH refers to in situ pH or to pH is referred to any temperature, pH is mostly temperature dependent, but also pressure. I understand that the pH decrease in the water column is calculated for in situ temperature and pressure. But I think it needs to be clearly stated.

In the revised manuscript, we will clarify that we always refer to in situ pH. This is standard practice for modellers. We will also mention the pH depends on temperature and pressure.

5) Section 3.2 Air-sea flux.

Please make clear that you refer to CANT air-sea fluxes and the way they are calculated: do you calculate the storage (inventory), the transport across the Strait and then the air-sea is derived from them, or the other way, the air-sea CANT flux and storage are calculated from the model and the transport across the Strait is derived from them.

In the revised manuscript, we will make it clearer that the text always refer to anthropogenic carbon for concentrations, fluxes and transport. We will also further clarify how things are calculated. In short, we directly simulate the air-sea flux of anthropogenic CO_2 and the build up of anthropogenic C_T. Inventories are calculated as vertical integrals of the latter. Lateral fluxes of anthropogenic carbon at the Strait of Gibraltar are computed from the model's advective fields and its simulated anthropogenic C_T. We have verified that the modeled storage of anthropogenic carbon (basin-wide inventory) is equal to the air-sea flux of anthropogenic carbon plus the net lateral transport across the Strait of Gibraltar. That is, the model conserves mass.

6) Section 3.3 Budget.

I understand in Fig. 8 that the light blue solid curve (inventory) is the sum of the green solid one (air-sea flux) plus the Gibraltar transport (solid purple). But I do not understand Fig. 9, what is the light blue dashed line (total storage) here?. I would plot the rate of change of the storage with time and the % contribution to it of the air-sea flux and the Gibraltar transport.

In the legend to Fig. 9, we will clarify (1) that the dashed purple line is the percent of total δC_T that outflows at the Strait of Gibraltar and (2) that total storage (light blue dashed line) is the percent of total δC_T that has entered Mediterranean Sea that remains in the Mediterranean Sea (total inflow minus Gibraltar outflow). The reviewer makes an interesting suggestion to plot instead of the cumulative change, the annual rate of change of the storage with time along with its contribution to the air-sea flux and Gibraltar transport. We will make this plot, and if it does indeed seem clearer, we'll include it in the revised manuscript.

7) Section 3.6 δpH.

It might be interesting to present the GLO results just to show that the MedSea is particular, but presenting the MED and VAR results as well it is a bit blurring. The consequence of smaller pH changes in warm waters with a higher TA is a direct consequence of the CO_2 chemistry, eastern MedSea waters have the lowest DIC/TA ratio and consequently are more resistant to changes due to a DIC increase due to air-sea CO2 exchange (DIC increase, TA constant). This is shown in Alvarez et al. (2014).

If we understand the first criticism correctly, the reviewer suggests that we show results only for the GLO simulation and either the MED or VAR results. We do not agree. We must discuss results from all three simulations in order to demonstrate the sensitivity of the pH change to alkalinity and to quantify the extent to which spatial variability of alkalinity matters.

Referee #1 is correct to point out that higher A_T implies a smaller rate of change of pH with respect to the CO_2 increase (∂pH/∂pCO_2). However, the difference is small as discussed below. Moreover, others have suggested just the opposite, that the Med Sea's higher alkalinity implies a higher rate of acidification (Touratier and Goyet, 2011).

In the revised manuscript, we will present additional analyses to adress this concern more quantitatively. As a start, we will show recently completed equilibrium calculations of

$\partial[H^+]/\partial pCO_2$. For more details, see our answers in section 11, Fig. 1 in this response). These calculations were made using the corrected equations from Egleston et al. (2010), made available as a new routine (buffesm) in the seacarb package by Orr (2011). They demonstrate that $\partial[H^+]/\partial pCO_2$ is only 8% lower in the eastern basin at its maximum A_T (2650 $\mu molkg^{-1}$) relative to the western basin's minimum A_T (2380 $\mu molkg^{-1}$). Slightly less than the western minimum is the global ocean's average alkalinity of 2300 $\mu molkg^{-1}$. These equilibrium rates will also be compared to those computed from model output.

In addition, we will focus on the change in $[H^+]$. The model's average simulated anthropogenic increase (1800–2001) in $[H^+]$ is only 1% less in the eastern relative to the western basin (VAR simulation in Table 1 below). One might expect then that the corresponding pH reduction would also be slightly less in the east, but it actually turns out to be slightly more (by 0.0004 units). That apparent discrepancy is really just due to taking differences on a log scale. Absolute differences in pH actually reflect a relative change in $[H^+]$; they depend on the initial state, which also differs between east and west. In any case, the difference is small, requiring 4 digits after the decimal to detect it.

The revised manuscript will further clarify the relationship between the rate of acidification and alkalinity. It will demonstrate quantitatively the extent to which the Mediterranean's acidification rate is less than the global ocean average.

I think is very simplistic the last phrase in this section. If the pH change is so similar with any model simulation why bother to perform them. I do not think is identical, I do think that the spatial variations matter. But I would also ask if the yearly temporal changes are comparable to the seasonal changes?.

From the context, it appears that the Referee is not actually referring to the last sentence in this section but the last sentence in the 3rd to last paragraph (p. 6486, lines 21–24): "Although the higher alkalinity of the Mediterranean Sea enhances its anthropogenic carbon content by 10%, the anthropogenic reduction in surface pH is not significantly different from that for typical surface waters of the global ocean." In the revised manuscript, we will change that sentence to, "The Mediterranean Sea's higher alkalinity, relative to the global-ocean average, enhances

its anthropogenic carbon content by 10% while reducing its average anthropogenic change in surface acidity ($[H^+]$) by 8%. However, the corresponding pH changes differ by only 0.001 unit, an artefact of taking differences on a log scale."

Regarding the seasonal cycle, we prefer to leave that to future work, particularly because seasonal variations may largely be dominated by the cycle of natural CO_2, which we do not model.

8) Section 4.1 δC_T in the MedSea.

I am not a TTD expert but I miss some details about the TTD setting in Schneider et al. (2010), although also discussed in this paper, the Δ/Γ ratio matters to calculate CANT. This ratio needs to be commented regarding the 2010 paper and the settings in the model.

In the revised manuscript, we will clarify what was done for the TTD approach. In particular, we will state that for consistency we have used exactly the same approach and settings as elaborated in Schneider et al. (2010). That allows a rigorous comparison of TTD δC_T estimates from CFC-12 measurements and model results. Both studies used $\Delta/\Gamma = 1$, which is appropriate for the interior ocean (Waugh et al., 2004).

9) Section 4.2 Transfer across the Strait of Gibraltar

Page 6481, lines 26-27: I totally disagree with this statement, in the global ocean the transport of CANT matters a lot, and there is a wealth of reference dealing with this point. This section is too long for the final conclusion achieved, it might be good to reduce the information given with numbers.

We do not understand why the Referee disagrees with the cited sentence (p. 6487, lines 26-27): "Unlike the global ocean where outside input of anthropogenic carbon comes only from the atmosphere, in the Mediterranean Sea there is also lateral input and output of anthropogenic carbon via the Strait of Gibraltar." We think this is obvious even without having made any simulation. Perhaps, the Referee is referring to another sentence? In any case, we certainly agree with her that the transport of δC_T matters a great deal, both in the global ocean and in the Mediterranean Sea; we never say otherwise. Our point on the source of the anthropogenic

carbon is important though. Whereas for the global ocean, all the anthropogenic carbon inventory comes from the air-sea CO_2 flux, in the Mediterranean Sea, 25% of the inventory comes from net transport across the Strait of Gibraltar. As for the length of this section, we will do our best to shorten it in the revised manuscript following the reviewer's recommendations.

10)

Section 4.3 Sensitivity to TA

As commented previously, using the better resolution of the M84/3 2011 data to constrain TA and the information given in other papers for the contribution of riverine TA would improve the model results. I think that discussing the GLO results is trivial. This section needs to be reduced.

We have already addressed the Referee's first remark in detail in previous responses. For the second remark, we do not understand why the Referee thinks that the GLO results are trivial. We think GLO is critical as a reference having the same total alkalinity everywhere as the mean for the global ocean. Only by comparison with the GLO simulation can we demonstrate how much the total alkalinity matters in terms of basin-wide uptake of anthropogenic carbon. We do not think that the results for the GLO simulation could have been guessed ahead of time, e.g., that its basin-integrated air-sea flux would be 25% lower than in the other 2 simulations, while its anthropogenic carbon inventory would be 9% less. For these reasons, we do not intend to reduce the length of this subsection, which takes up only 3.5 short paragraphs.

11) Section 4.4 Change in pH.

Page 6486, line 2-4: sorry to say, but your sensitivity test do not demonstrate anything, the direct consequence of the low DIC/TA ratio in the eastern MedSea is the lower change in pH (due to air-sea CO2 exchange) compared to waters with a higher DIC/TA ratio, this is shown in Alvarez et al with the 2011 data, but is a direct consequence of the CO2 chemistry, anybody could simulate this using DIC, TA, Temp and salinity from the MedSea.

If the referee failed to see the interest of our sensitivity tests, then we failed in communicating it. In the revised manuscript, we will take on this challenge while relying on a new, more targeted analysis of how the acidification rate is affected by total alkalinity as well as other key factors,

temperature, salinity, and the air-sea disequilibrium. In the sentence referred to by Referee #1, we stated that "the higher total alkalinity of the Mediterranean Sea does not result in a greater anthropogenic reduction in surface pH." We admit that they are not exactly identical but they are very close. In the revised manuscript, we will be more quantitative and discuss the change in H^+ as well as pH. For the latter, basin-wide means in our 3 simulations are identical to 2 decimal places (as listed in a new Table, given below as Table 1).

Our enhanced assessment will clarify precisely how much the rate of acidification ($\partial[H^+]/\partial pCO_2$) of the Mediterranean Sea differs because of its higher alkalinity. For simplicity, we will first show equilibrium calculations of $\partial[H^+]/\partial pCO_2$ using analytical equations of Egleston et al. (2010) as corrected by Orr (2011), as detailed in his contribution of the 'buffesm' routine of the seacarb carbonate system software package. A new figure will be shown with $\partial[H^+]/\partial pCO_2$ that was calculated by varying alkalinity from the minimum observed in the western basin (2380 μmol kg^{-1}) to the maximum observed in the western basin (2650 μmol kg^{-1}) and assuming equilibrium with atmospheric CO_2. Temperature and salinity were held at the minimum values observed in the western basin during summer.

The Mediterranean's west-to-east increase in alkalinity alone reduces $\partial[H^+]/\partial pCO_2$ by 8% (see new figure below, referred to here as Fig. 1). Then after including the west-to-east temperature increase (6°C during summer) the $\partial[H^+]/\partial pCO_2$ is reduced by another 0.5% (i.e., for the east relative to the west). But the temperature reduction in $\partial[H^+]/\partial pCO_2$ is compensated by the west-to-east increase in salinity (3 units on the practical salinity scale) during summer. For comparison, there is a 2% decrease in $\partial[H^+]/\partial pCO_2$ as atmospheric xCO_2 increases from 280 to 385 ppm and another 4% decrease when atmospheric xCO_2 increases further to 850 ppm.

The model's surface acidification rates are slightly less intense, because it does not make the simplification that atmospheric and oceanic pCO_2 are identical (i.e., in equilibrium). Another new figure shown below (Fig. 2 in this response) shows the model's average simulated $\partial[H^+]/\partial pCO_2$ per band of longitude (meridional mean) both in 1800 and in 2001 for each of the 3 simulations. It also shows the corresponding change in $[H^+]$ (nmol kg^{-1}). The acidification rate is 8% lower in MED ($\sim$17.5 pmol kg^{-1} μatm^{-1} in 2001) than in GLO ($\sim$19.1 pmol kg^{-1} μatm^{-1} in 2001). In VAR, the $\partial[H^+]/\partial pCO_2$ decreases by 8% in 2001 when moving from

west to east (from ∼18.5 to ∼17 pmol kg^{-1} μatm^{-1}). That modeled west-to-east gradient is much like that found with the thermodynamic calculations, but curves are displaced downwards by 0.3 units.

The higher alkalinity of the Mediterranean Sea, relative to the global ocean, reduces its anthropogenic change in acidity ($[H^+]$) by 9% on average, but the average change in the eastern basin is only 1% lower than that in the western basin (Table 1 below). The latter is less even than estimated by the equilibrium calculations. The Referee was right to emphasize that there are differences in rates of acidification due to alkalinity. In the revised manuscript, we will demonstrate that the differences are small.

Referee #1's final point that anyone could determine the effect of alkalinity on the acidification rate should be nuanced. Certainly almost anyone could make equilibrium calculations, but few have. Perhaps only two studies have touched on the issue with respect to the Mediterranean Sea (Orr, 2011; Alvarez et al., 2014). We are the first to discuss model simulations in the Mediterranean Sea, which do not assume air-sea equilibrium and take into account other physical factors that equilibrium calculations cannot. Moreover, opposite conclusions from others (Touratier and Goyet, 2011) point to a general lack of understanding surrounding this issue. We hope that our revised manuscript will help close the debate.

References

Álvarez, M., Sanleón-Bartolomé, H., Tanhua, T., Mintrop, L., Luchetta, A.,Cantoni, C., Schroeder, K., Civitarese, G.: The CO_2 system in the Mediterranean Sea: a basin wide perspective, Ocean Science, 10, 69–92, 2014, doi:10.5194/os-10-69-2014

Egleston, E. S., Sabine, C. L., and Morel, F. M. M.: Revelle revisited: Buffer factors that quantify the response of ocean chemistry to changes in DIC and alkalinity, Global Biogeochem. Cycles, 24, GB1002, doi:10.1029/2008GB003407, 2010

Orr, J. C.: Recent and future changes in ocean carbonate chemistry, in: Ocean Acidification, edited by: Gattuso, J. and Hansson, L., Oxford University press, Oxford, 41–66, 2011.

Schneider, A., Wallace, D. W. R., and Körtzinger, A.: Alkalinity of the Mediterranean Sea, Geophys. Res. Lett., 34, L15608, doi:10.1029/2006GL028842, 2007.

Schneider, A., Tanhua, T., Körtzinger, A., and Wallace, D. W. R.: High anthropogenic carbon content in the eastern Mediterranean, J. Geophys. Res., 115, C12050, doi:10.1029/2010JC006171, 2010.

Touratier, F. and Goyet, C.: Impact of the Eastern Mediterranean Transient on the distribution of anthropogenic CO_2 and first estimate of acidification for the Mediterranean Sea, Deep-Sea Res. Pt. I, 58, 1–15, doi:10.1016/j.dsr.2010.10.002, 2011.

Waugh, D. W., Haine, T., Hall, T. M.:Transport times and anthropogenic carbon in the subpolar North Atlantic Ocean, Deep-Sea Res. Pt. I, 51, 1475–1491, 2004, doi:10.1016/j.dsr.2004.06.011

Table 1. Average changes in pH and $[H^+]$ between 1800 and 2001 for the three simulations for the Mediterranean Sea and its western and eastern basins.

	δpH			$\delta[H^+]$ (nmol kg^{-1})		
	West	East	Med Sea	West	East	Med Sea
GLO	-0.0851	-0.0849	-0.0850	1.45	1.46	1.46
MED	-0.0823	-0.0848	-0.0840	1.29	1.35	1.33
VAR	-0.0833	-0.0837	-0.0836	1.33	1.32	1.32

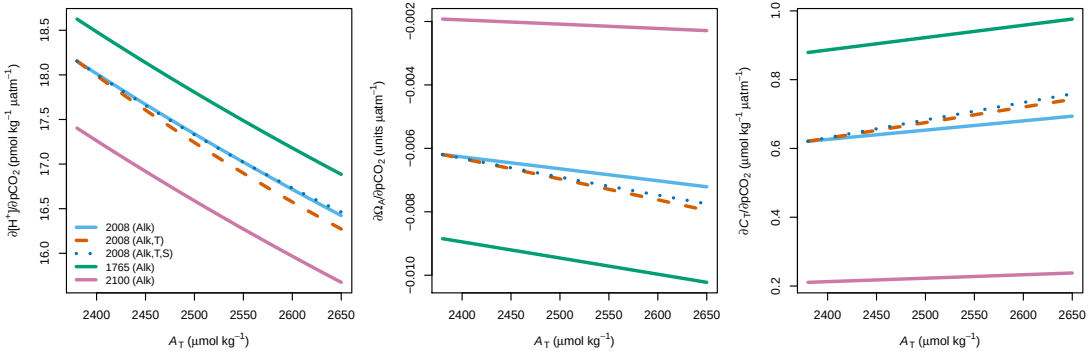

Figure 1. Acidification rate ($\partial[H^+]/\partial pCO_2$, in pmol kg^{-1} μatm^{-1}) as a function of alkalinity varied over the observed Mediterranean range (2380 to 2650 μmolkg^{-1}) for 3 different atmospheric xCO_2 levels in 1765 (280 ppm, solid light-blue line), 2008 (385 ppm, solid green line) and 2100 (850 ppm, solid purple line) Also shown are lines for 2008 to illustrate the effects of also varying temperature (dashed orange) and temperature and salinity (dotted blue) over the observed west-to-east range.

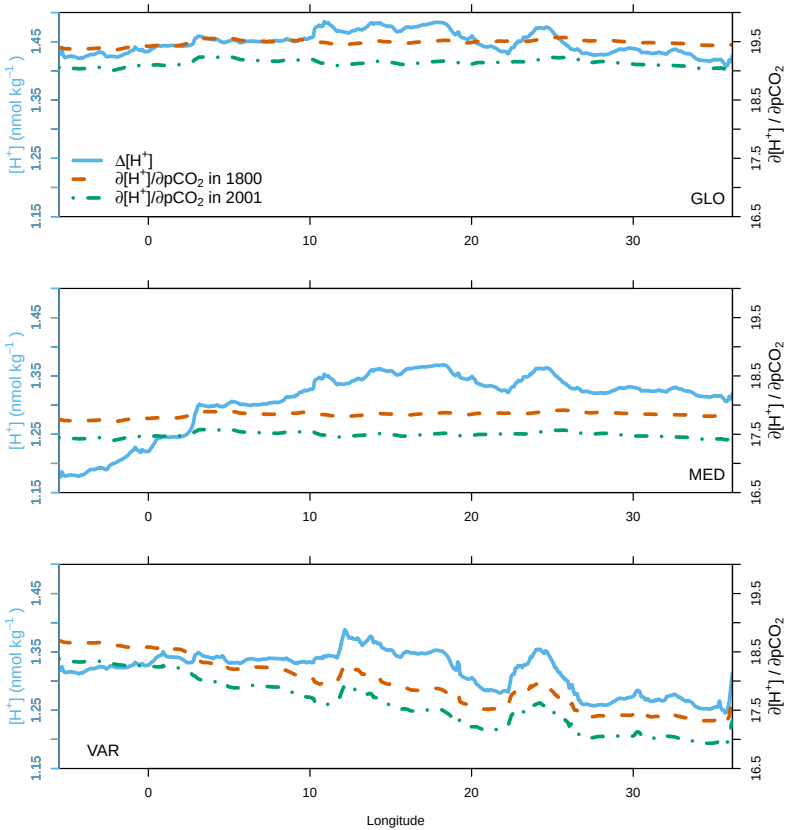

Figure 2. Meridional mean of the acidification rate $\partial[H^+]/\partial pCO_2$ in pmol kg^{-1} μatm^{-1}) in 1800 (dashed orange) and in 2001 (dashed-dotted green) in the Mediterranean Sea along with the corresponding $[H^+]$ change between 1800 and 2001 in nmol kg^{-1} (solid light-blue). Meridional means are taken from all grid cells with salinities above 32, thus avoiding bias from river mouths.

Manuscript prepared for Biogeosciences Discuss.
with version 2014/05/30 6.91 Copernicus papers of the LaTeX class copernicus.cls.
Date: 29 July 2014

Simulated anthropogenic CO_2 uptake and acidification of the Mediterranean Sea

J. Palmiéri[1,2], J. C. Orr[1], J.-C. Dutay[1], K. Béranger[2], A. Schneider[3], J. Beuvier[4,5], and S. Somot[5]

[1]LSCE/IPSL, Laboratoire des Sciences du Climat et de l'Environnement, CEA-CNRS-UVSQ, Gif-sur-Yvette, France
[2]ENSTA-ParisTech, Palaiseau, France
[3]GEOMAR; Helmholtz-Zentrum für Ozeanforschung Kiel, Germany
[4]Mercator Ocean, Ramonville Saint-Agne, France
[5]CNRM/Météo-France, Toulouse, France

Correspondence to: J. Palmiéri (julien.palmieri@lsce.ipsl.fr)

1 Response to Referee #2

We thank Referee #2 for constructive comments, which have helped improve the manuscript. Below the Referee comments are repeated (in gray) and our responses follow (in black).

1.1)

This paper discusses model results from a model that simulates the ventilation and circulation of the Mediterranean Sea, with emphasis on two passive tracers (CFC-12 and DIC). The paper does a careful and very nice comparison of model results to data based results. It also calculates fluxes of anthropogenic carbon through the Strait of Gibraltar, and draw relevant conclusions on the ocean acidification of the Mediterranean Sea. The paper is very well written and an effort to join model and observational estimates in a common frame-work. The paper certainly merits publication in BG.

Many thanks for these positive remarks.

However, I do have some concerns about the model / data comparison that needs serious attention, and a number of minor suggestions that should be easy to correct. The most serious considerations concerns 1) the comparison of data based TTD derived estimates with the modeled deltaDIC and TTD(MW), and 2) the conclusion of the lower limit for Cant storage in the Mediterranean Sea. 1) I wonder why the model have 10 umol/kg lower Cant in the surface (section 3.5). The TTD method assumes (per definition) that the age of the surface water is zero, and the anthropogenic carbon content is only a matter of thermodynamics with a given alkalinity, temperature and pCO2. The 68 umol/kg of surface Cant is roughly what you would expect from thermodynamic considerations of the carbonate system. This suggests to me that the model finds kinetic restrictions to the saturation of Cant so that the air-sea equilibrium has changed over the anthropogenic time-period with roughly 15%. Can you verify or comment on this. It is surprising that such a large deltadeltapCO2 is found.

Data-based methods such as TTD do indeed assume that the change in ocean pCO_2 is identical to the change in atmospheric pCO_2. But this assumption must be wrong in the real ocean. If it were true, then the air-sea difference ($\Delta\delta pCO_2$) must always be zero, which implies that the air-sea flux of anthropogenic CO_2 must likewise be zero (see equation 5 in our submitted

manuscript). Certainly, the anthropogenic CO_2 flux cannot be zero given that all data-based and modeling approaches indicate that the ocean does indeed contain substantial amounts of anthropogenic C_T.

The notion that the ocean $p\mathrm{CO}_2$ increase exactly follows that in the atmosphere, comes in part from measured or calculated $p\mathrm{CO}_2$ at 3 time-series stations (BATS, HOT, and ESTOC), where calculated atmospheric and oceanic trends are not significantly different (Bindoff et al., 2007). However, these stations are all located in subtropical gyres where both the air-sea flux of anthropogenic CO_2 and the corresponding air-sea disequilibrium are the lowest (Figure 2 in Sarmiento et al. (1992)). In short, the subtropical gyres are the worst place to look if one is trying to detect a non-zero air-sea disequilibrium ($\Delta\delta\mathrm{pCO}_2$); it would be much better to look in the high latitudes, such as in the Southern Ocean. Although data-based methods that estimate anthropogenic C_T in the ocean find it convenient to assume that $\Delta\delta\mathrm{pCO}_2 = 0$, it has been recognized for years by some members of that community that that basic assumption does not hold in the real ocean (Orr et al., 2001). The lingering question then is how much of an error does that erroneous assumption imply? We think our simulations and particularly our tests of TTD in the model world offer a quantitative response for the Mediterranean Sea.

The reviewer is correct that our model's air-sea disequilibrium reaches 15% and even more in some places. In terms of the air-sea difference in $\delta\mathrm{pCO}_2$, our $\Delta\delta\mathrm{pCO}_2$ varies between 14 and 20 ppm in 2001, equivalent to the ocean $p\mathrm{CO}_2$ increase lagging that in the atmospheric by 20% since 1850 (Fig. 1 in this response). But we do not find those numbers surprising. They fall well within the 6-to-40 ppm range estimated by a global model (Figure 2 in Sarmiento et al. (1992)).

1.2)

Why do you conclude that the TTD(MW) is an overestimate, and not the other way around (i.e. the deltaDIC from the model) an underestimate? I am not saying that is the case, but it is strange to me that the model is able to reproduce the surface CFC-12 concentrations very well, but the TTD(MW) is still lower than the observational based TTD values? Are you using the

same routines and supporting variable values for these calculations? The base of this question is: why is the TTD(data) different from the TTD(MW) when the CFC-12 values are the same?

We think that the TTD approach in the model world provides an overestimate of the δDIC because it assumes that the air-sea disequilibrium in anthropogenic CO_2 is null ($\Delta\delta pCO_2 = 0$), as elaborated above. That is, its oceanic δpCO_2 is too high, making its δDIC too high. There is no evidence to suggest that at the surface the simulated δDIC is too low (inconsistent with the model world circulation, ocean chemistry, and atmospheric CO_2). The chemistry is straightforward and well constrained, following best practices. The simulated flux of anthropogenic CO_2 is relatively insensitive to the gas exchange coefficient (Sarmiento et al., 1992). Ocean biology does not play a role, by definition. In the revised version of the manuscript, we will thoroughly discuss these concerns raised by Referee #2.

As described in the manuscript, coefficients for our perturbation approach were derived using the same carbonate chemistry routine (carb from seacarb) with the set of constants recommended for best practices, as used in our simple tests that assumed thermodynamic equilibrium.

Actually, the δC_T estimated by applying the TTD approach in model world (TTD(MW)) is similar to the TTD estimate of δC_T from observational data (TTD(data)) as shown in Fig. 2 (in this response) when CFC-12 concentrations are similar. In those cases, differences remain less than 10%.

2) We know that the model underestimates the strength of the deep overturning circulation in the Mediterranean from the too low CFC-12 values in the model. The model is roughly half of the observations over close to 2000 meter depth interval. Presumable the too low CFC-12 concentration in the model corresponds to a too low Cant concentration in the model. However, no attempt is made to quantify this difference. I can imagine many ways to do this, from "tuning" the model to match observations (of CFC-12), or more simple calculations based on relationship between CFC-12 and Cant for the Med. At any rate this should be done for the model Cant inventory calculations. As it stands now you present a value of Cant that you KNOW is an underestimate and state since this is lower than the TTD(data) estimate, the TTD(data) estimate has to be an upper limit. You might be correct with that statement, but it is not proven with the

current data. Also, the point brought up above (1) suggest that the model Cant inventory is an underestimate by even more than the too low CFC-12 values suggest. These two points requires some careful analysis and discussion, and might have implications for discussion on pH and flux through the Strait of Gibraltar.

In the revised manuscript we will offer a more careful analysis and discussion. For now, let us try to clarify what seems to us as misunderstandings of our approach and our conclusions.

Concerning our approach, we simulate CFC-12 and compare it to observations to evaluate the simulated circulation, particularly the model's ventilation of deep waters. That is standard practice in the modeling community. Our goal was never to use the CFC-12 data to actually adjust and tune the model. Tuning a general circulation model is a huge task, unlike simple box models. To do what is suggested by Referree #2, tuning our general circulation model with the CFC-12 data, would require implementing an adjoint or inverse approach. Moreover, it would change the overall approach from being prognostic (predictive) to being diagnostic. For our simulations, the model must be prognostic, i.e., free to be perturbed by realistic, interannually varying boundary conditions (e.g., heat and water fluxes as well as wind fields). Furthermore, an inverse approach typically alters temperatures and salinities below the surface, necessarily with subsurface artificial additions or subtractions of heat and salt which are completely unphysical. For these reasons then, we stay with prognostic modeling approach for this study.

Although both CFC-12 and anthropogenic CO_2 can be treated as passive, transient tracers, they have different solubilities, air-sea equilibration times, atmospheric histories, and penetration depths. Hence we consider it inappropriate to adjust simulated δC_T results by using CFC-12 results. Philisophically, we think it is of greater value to know that a model is a lower limit than to try to adjust it in inexact ways to be a "best estimate" with unknown uncertainties and biases. Bracketting the real behavior seems more rigorous to us than to go for a best estimate.

As for our conclusions, unlike what is stated by Referee #2, we do not consider that TTD(data) is an upper limit just because its estimates are higher than those from the model. Rather, we consider that TTD overestimates $\delta \mathrm{C}_T$ because in the model world it overestimates simulated anthropogenic C_T. Furthermore, we know that at least part of the cause is that TTD assumes $\Delta\delta p\mathrm{CO}_2 = 0$. That the latter must be non-zero can be demonstrated by even the sim-

plest of box models with finite gas exchange, and by the basic equation $F = \mathrm{kg}\,\Delta\delta p\mathrm{CO}_2$, as discussed previously.

We will do our best to clarify the misunderstandings raised by Referee #2 in the revised manuscript.

Specific comments:

Abstract and possibly elsewhere: Are you referring to uptake (as in air-sea exchange) or to increased interior storage of DIC? The term uptake is maybe not what you want to say, please check and modify. Maybe storage would be a better word to use.

Good point. We will clarify differences between storage and uptake in the revised manuscript.

Page 6464, line 18:I am not sure the "south of" is correct here. I suggest to leave that out since the deep water is/was actually formed in the Adriatic and in the Aegean (including south of the Aegean during the EMT).

Good advice, which we will follow in the revised manuscript.

Figure 1: The sections of the two Cant estimates are identical, so why is the average profile of TrOCA much more shallow than the TTD profile? Please make them comparable.

The average profile of TrOCA is much shallower the that of TTD on each section because the TrOCA method requires more variables to make the computation; TTD only needs CFC-12. That is, some of TrOCA input variables were not available in the deeper bottles. We will clarify the cause of this difference in the revised manuscript.

Supplementary material: I do appreciate that you publish the scripts used for the calculations and the constants. However, please put some effort into making this easily readable in a pdf version as well (keep the dat and R files since I assume they can be directly read by the code).

We will provide a listing of the R script as a PDF file and include that in the Supplementary Material of the revised manuscript.

I could not find table A1, for instance.

Table A1 refers to that in Wanninkhof (1992), not ours. We used the standard approach to cite an already published table (Wanninkhof 1992, Table A1), as advised in the Guide to Authors. If there is a better way, we would be happy to change our text.

Page 6471, line 20: Please remove "exactly", same for page 6473, line 5.

We will remove "exactly" from the revised manuscript.

Page 6474, line 11: Do you mean that the DIC was in equilibrium with the atmosphere, rather than the alkalinity? Please reformulate.

Thanks for pointing out this confusion. We meant that for the purposes of our perturbation apporach, we assume that preindustrial C_T is in thermodynamic equilibrium with both prescribed surface alkalinity and atmospheric xCO_2. We will clarify this point in the revised manuscript.

Section 3.4: Would it be appropriate to call this section "modelled deltaCT inventory"?

Good suggestion. In the revised manuscript, we will rename this section to "Simulated δC_T inventory".

Page 6478, line 25: Please state that (again) that you are referring to modelling "data" wrt poor ventilation; the observations seems to be different.

We do not understand why this sentence is confusing to the Referee. We state that "let us simply compare model results to the TTD data-based estimates of δC_T estimated from observations". Nonetheless, we will try to clarify further in the revised manuscript.

Section 3.5: I had some problems keeping the "model underestimate the data based estimates" terminology in this section. Maybe it would help rephrasing (on several occasions) to state "the model deltaCT is lower than the data based TTD results", or something like that.

This rephrasing does seem an improvement and will be considered more generally for the revised manuscript.

Page 2478,line 25: change " estimated from" to " based on".

In the revised manuscript, we will make this change as well as remove "data-based" to avoid redundancy.

Section 3.6: The low Cant in the modelled surface, see above discussion on low Cant in the surface, also impact this discussion that might need to be reconsidered.

We will modify this discussion to clarify the general points we have made above about the comparison of simulated δC_T with the corresponding TTD data-based estimates.

Figure 14: Please change legend in the right hand panel to "deltaDIC TTD(MW)"

We will make this change in the revised manuscript.

Page 6488, line 3: add "poorly ventilated vs. observations- It could be appropriate to cite studies comparing various data based Cant estimates somewhere in the discussion where the TrOCA, DeltaC* and TTD results are compared (for instance (Yool et al., 2010;Álvarez et al., 2009;Vázquez-Rodríguez et al.,2009)).

In the revised manuscript, we will cite these studies, although they did not include comparison of these techniques applied to data in the Mediterranean Sea. In the Med Sea there is generally larger disagreement, e.g., between TTD and TrOCA (see Fig. 1 in the submitted manuscript).

References

Bindoff, N. L., Willebrand, J., Artale, V., Cazenave, A., Gregory, J. M., Gulev, S., Hanawa, K., Le Quéré, C., Levitus, S., Nojiri, Y., Shum, C. K., Talley, L. D., and Unnikrishnan, A. S.: Observations: Oceanic climate change and sea level, in Climate Change 2007: The Physical Science Basis. Contribution of Working Group I to the Fourth Assessment Report of the Intergovern- mental Panel on Climate Change, edited by S. Solomon et al., chap. 5, Cambridge University Press, Cambridge, United Kingdom and New York, NY.

Orr, J. C., Monfray, P., Maier-Reimer, E., Mikolajewicz, U., Palmer, J., Taylor, N. K., Toggweiler, J. R., Sarmiento, J. L., Le Quere, C., Gruber, N, Sabine, C. L., Key, R. M., and Boutin, J.: Estimates of anthropogenic carbon uptake from four threedimensionsal global ocean models, Global Biogeochem. Cycles, 15, 43–60, 2001.

Sarmiento, J. L., Orr, J. C., and Siegenthaler, U.: A perturbation simulation of uptake in an ocean general circulation model, J. Geophys. Res., 97, 3621–3645, 1992.

Wanninkhof, R.: Relationship between wind speed and gas exchange over the ocean, J. Geophys. Res., 97, 7373–7382, 1992, doi:10.1029/92JC00188

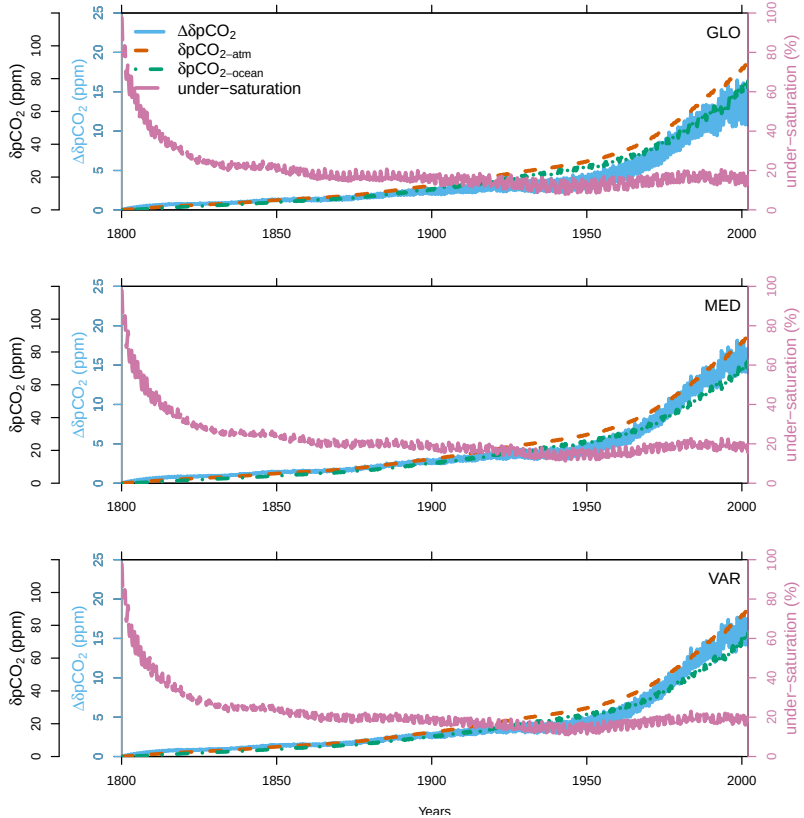

Figure 1. Temporal evolution from 1800 to 2001 of spatially avarage δpCO$_2$ (in ppm) in the atmosphere (dashed orange), the ocean (dashed-dotted green), and their difference difference $\Delta\delta$pCO$_2$ (solid light-blue line). Also shown is the corresponding percent undersaturation of oceanic δpCO$_2$ (long dashed purple), defined as $100\left(1-\left(\frac{\delta pCO_{2\,oc}}{\delta pCO_{2\,atm}}\right)\right)$.

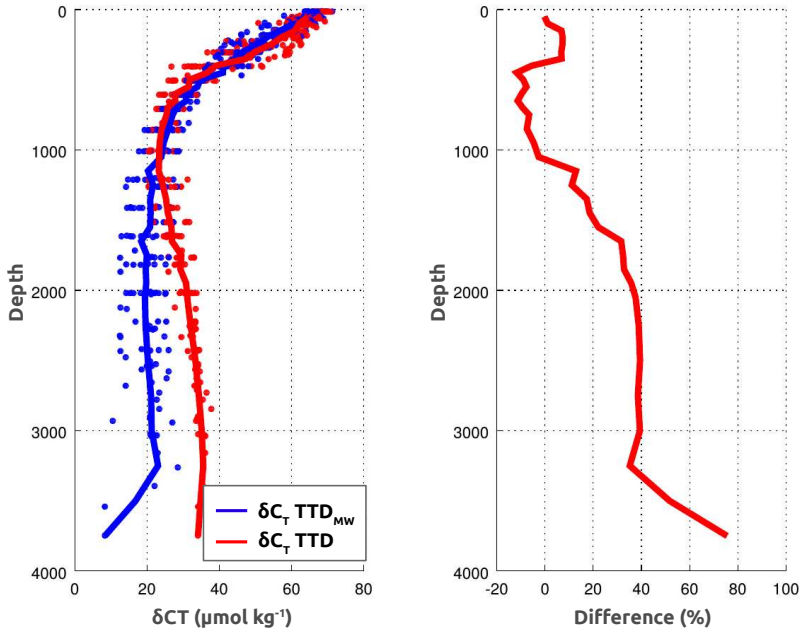

Figure 2. Average profiles of δC_T from the TTD approach using model results (TTD_{MW}, blue) and observational data (TTD, red). Shown are (left) all data (and corresponding model output) along the METEOR 51/2 section (points) and averages (solid lines), and (right) the percent difference betweeen the two averages.

Palmiéri et al., 2014 -
Simulated anthropogenic CO_2 uptake and acidification of the Mediterranean Sea.

Detailed corrections list, that correspond to the reviewers' questions and remarks: (page and line correspond to pages and lines of the submission version of the paper).

1. changed "uptake" to "storage" in the title, the abstract and in the introduction

2. Page 6464 – line 18 – removed “south of”.

3. Page 6473 – line 7 – explain that our carbonate chemistry model takes into account Temperature and salinity changes : " Carbonate chemistry simulated by the model is hence sensible to the spatial and temporal evolution of T in GLO and MED experiments (in the calculation of z0 and z1 coefficients), and of T and S in the VAR experiment (Eq. (12))".

4. Page 6473 – line 15 to 20 – Explain what a simulation off-line is, and try an easier explanation of looping through the circulation fields. We also have removed the corresponding Figure 4, that did not helped in the explanation.

5. Page 6474 – line 9 – add a precision that pH always refer to in-situ pH

6. Page 6474 – line 10 – change the sentence from "The preindustrial C_T was computed by assuming that the prescribed total alkalinity was in thermodynamic equilibrium with an atmospheric xCO_2…" to "The preindustrial C_T was computed by assuming it in thermodynamic equilibrium with the prescribed total alkalinity and with an atmospheric xCO_2 ...".

7. Page 6476 – line 4 – we clarify that air-sea flux are air—sea flux of anthropogenic carbon, and that they are directly calculated by the model.

8. Page 6478 – line 1 – changed the name of section 3.4 to Simulated δC_T inventory

9. Page 6478 – line 19 – changed the name of section 3.5 to Comparison with TTD data-based results.

10. Page 6478 – line 25 – removed "data-based"

11. Page 6478 – line 25 – changed from "estimated from" to "based on"

12. Page 6478 – line 27 – changed from " the model underestimates everywhere the TTD data-based" to " the model δCT is everywhere lower than the TTD"

13. Page 6479 – line 4 – changed from " the model is seen to underestimate the data-based estimates" to " the model δCT is seen to underestimate the TTD results"

14. Page 6479 – line 17 – change from "Relative to the data-based estimates" to "Relative to the data-based TTD results"

15. Page 6479 – line 20 – removed "data-based"

16. Page 6479 – 6480 – section 3.6: reevaluated all δpH values, with best practice estimates.

17. Page 6481 – line 5 – clarify the TTD approach version and parameters used in the model world experiment.

18. Page 6481 – line 18 – added a paragraph to explain why we conclude that TTD approach overestimates the Mediterranean anthropogenic carbon. We also added a Figure (new Fig. 14) to illustrate the air—sea δCO_2 disequilibrium.

19. Page 6486 – section 4.4 – this section have been modified to answer referee #1 remark over Mediterranean high alkalinity effect on the anthropogenic change of Mediterranean water pH. We have added a table that compare Mediterranean sea pH change in the whole Med sea, the Eastern basin and in the western basin, and the equivalent change in $[H^+]$ ions. We also have changed our equilibrium test to highlight Mediterranean sea's specific acidification rate, and distinguish the effect of alkalinity, temperature, and salinity on this acidification rate. Then we have added another picture that shows a meridional average of the Mediterranean acidification rate in 1800 and in 2001 for both 3 simulations, and the equivalent change in $[H^+]$ ions.

20. Page 6488 – line 2 – added "compare to observations"

21. Fig. 1 – added " (Note that the vertical profile of the TrOCA method does not go below 3500m depth because it needs measurements some of which where not available at that depth)".

22. Fig. 7 – Figure has been replotted with R software, and the calculation procedure for air-sea flux, Gibraltar input and output fluxes, and total storage have been clarified.

23. Fig. 8 – Figure have been replotted with R software, and we changed from cumulative δC_T uptake, to the annual averaged uptake, and its air-sea/strait of Gibraltar flux contribution.

24. Fig. 10 – has been replotted with R software.

25. Fig. 13 – the legend in the right panel has been corrected.

26. The supplementary materials has also been improved with 2 notebook pages that explain how the coefficients of the carbonate chemistry model have been calculated.

artOrr2001artOrr2001432001Orr et al.Orr, Monfray, MaierReimer, Mikolajewicz, Palmer, Taylor, Toggweiler, Sarmiento, Le Quere, Gruber, Sabine, Key, and Boutin
Manuscript prepared for Biogeosciences Discuss.
with version 2014/05/30 6.91 Copernicus papers of the LaTeX class copernicus.cls.
Date: 27 October 2014

Simulated anthropogenic CO_2 ~~uptake~~ storage and acidification of the Mediterranean Sea

J. Palmiéri[1,2], J. C. Orr[1], J.-C. Dutay[1], K. Béranger[2], A. Schneider[3], J. Beuvier[4,5], and S. Somot[5]

[1]LSCE/IPSL, Laboratoire des Sciences du Climat et de l'Environnement, CEA-CNRS-UVSQ, Gif-sur-Yvette, France
[2]ENSTA-ParisTech, Palaiseau, France
[3]GEOMAR; Helmholtz-Zentrum für Ozeanforschung Kiel, Germany
[4]Mercator Ocean, Ramonville Saint-Agne, France
[5]CNRM/Météo-France, Toulouse, France

Correspondence to: J. Palmiéri (julien.palmieri@lsce.ipsl.fr)

Abstract

Constraints on the Mediterranean Sea's ~~uptake~~ storage of anthropogenic CO_2 are limited, coming only from data-based approaches that disagree by more than a factor of two. Here we simulate this marginal sea's anthropogenic carbon ~~uptake~~ storage by applying a perturbation approach in a high-resolution regional model. Our model simulates that between 1800 and 2001, basin-wide CO_2 ~~uptake~~ storage by the Mediterranean Sea has increased by 1.0 Pg C, a lower limit based on the corresponding model evaluation with CFC-12, indicating inadequate simulated deep-water ventilation. Furthermore, by testing a data-based approach (Transit Time Distribution) in our model, comparing simulated anthropogenic CO_2 to values computed from simulated CFC-12 and physical variables, we conclude that the associated basin-wide ~~uptake~~ storage of 1.7 Pg, published previously, must be an upper bound. Out of the total simulated ~~uptake~~ storage of 1.0 Pg C, 75 % comes from ~~air–sea~~ air-sea exchange into the Mediterranean Sea and 25 % comes from net transport from the Atlantic across the Strait of Gibraltar. Sensitivity tests indicate that the Mediterranean Sea's higher total alkalinity, relative to the global-ocean mean, enhances the Mediterranean's total inventory of anthropogenic carbon by 10 %. Yet the corresponding average anthropogenic change in surface pH does not differ significantly from the global-ocean average, despite higher total alkalinity. In Mediterranean deep waters, the pH change is estimated to be between -0.005 and -0.06 pH units.

1 Introduction

The Mediterranean region will be particularly affected by climate change (Giorgi, 2006; The MerMEX group, 2011; Diffenbaugh and Giorgi, 2012). This region, currently classified as semiarid to arid, is projected to become warmer and drier (Gibelin and Déqué, 2003; Giorgi and Lionello, 2008) amplifying existing water resource problems. At the same time, already heightened anthropogenic pressures are expected to intensify further (Attané and Courbage, 2001, 2004). It has been proposed that the Mediterranean Sea will experience amplified acidification relative to the global average surface ocean (Touratier and Goyet, 2009, 2011). The

Mediterranean Sea is able to absorb relatively more anthropogenic CO_2 per unit area for two reasons: (i) its higher total alkalinity gives it greater chemical capacity to take up anthropogenic CO_2 and neutralize acid and (ii) its deep waters are ventilated on relatively short time scales, allowing deeper penetration of this anthropogenic tracer. However the quantity of anthropogenic CO_2 that has been absorbed by the Mediterranean Sea remains uncertain. This quantity cannot be measured directly because the anthropogenic component cannot be distinguished from the much larger natural background. Instead it has been estimated indirectly from observable physical and biogeochemical quantities.

Several indirect methods have been developed, some of which have been compared using the same data sets along basin-wide transects in the Mediterranean Sea. Their first comparison (El Boukary, 2005) revealed large differences between methods. With data from a 1995 transect on the METEOR (M31/1), El Boukary estimated with two methods that the Mediterranean Sea has absorbed 3.1 and 5.6 $\mathrm{Pg\,C}$, but he concluded that even the lower value was an overestimate. Later, data from a transbasin transect in 2001 (METEOR M51/2) was used by two independent studies to estimate anthropogenic CO_2. In the first, Schneider et al. (2010) used that data with the Transit Time Distribution approach (TTD from Waugh et al., 2006), a back calculation method based on CFC-12 derived mean age of water masses. For the second, Touratier and Goyet (2011) used their TrOCA (Touratier et al., 2007) approach that relies on measured O_2, dissolved inorganic carbon (C_T), and total alkalinity (A_T). Anthropogenic carbon estimated with TrOCA is always greater than that from TTD (Fig. 1), with more than a factor of two difference both in the Western basin below 500 m depth and in the Eastern basin between 500 and 1500 m. These large differences in estimated concentrations further result in opposing estimates for the net transport across the Strait of Gibraltar. With TROCA, the Mediterranean Sea appears to export anthropogenic carbon to the Atlantic Ocean, whereas with TTD, net calculated exchange is in the opposite direction (Schneider et al., 2010; Aït-Ameur and Goyet, 2006; Huertas et al., 2009; Flecha et al., 2011). These large discrepancies between results from currently used data-based methods fuel a debate about the quantity of anthropogenic carbon that is taken up by the Mediterranean Sea.

Here we take another approach by simulating anthropogenic CO_2 ~~uptake~~ storage of the Mediterranean Sea. Unlike simulations for the global ocean, we cannot rely on coarse-resolution global models because they do not resolve fine-scale bathymetry and circulation features that are critical for the Mediterranean Sea. This semi-enclosed marginal sea is separated into the eastern and the western basins by the Strait of Sicily (Fig. 2). Each of these basins has critical circulation features that are often heavily influenced by bathymetry. For example, Atlantic Water (AW) enters the Mediterranean Sea at the surface via the narrow Strait of Gibraltar and flows counter-clockwise along the coast. Surface-water circulation patterns are influenced by deep- and intermediate-water formation driven by strong winds, which are themselves steered and intensified by surrounding mountainous topography. Deep and intermediate waters are formed in 4 major areas: the Rhodes gyre, where the Levantine Intermediate Water (LIW) originates; the Gulf of Lions and the nearby Ligurian Sea in the Liguro-Provençal sub-basin, which together produce Western Mediterranean Deep Water (WMDW); and two adjacent regions, ~~south of the Adriatic Sea and south of the adjacent Aegean Sea~~the Adriatic and the Aegean sub-basins, which together produce Eastern Mediterranean Deep Waters (EMDW). Also influencing the deep circulation is the Mediterranean Outflow Water (MOW), a complex mixture of different intermediate and deep waters outflowing at the Strait of Gibraltar underneath the incoming AW.

To capture these and other key features, we used a high-resolution circulation model of the Mediterranean Sea forced by high resolution ~~air–sea~~ air-sea fluxes, interannually varying Atlantic Ocean boundary conditions, and realistic land freshwater inputs. This regional circulation model is combined with a computationally efficient perturbation approach (Sarmiento et al., 1992) to model anthropogenic CO_2 in the Mediterranean Sea. This geochemical approach simulates only the change in CO_2 uptake due to anthropogenic perturbation, assuming that the natural carbon cycle is unaffected by the increase in CO_2. For efficiency, it relies on a formulation that relates surface-water changes in the partial pressure of carbon dioxide (δpCO_2) to those in dissolved inorganic carbon (δC_T). By focusing only on the C_T perturbation, it needs just one tracer and one simulation that covers only the industrial period. Thus it circumvents the need for the prequisite simulation of the natural carbon cycle, which requires many tracers and a much longer simulation to allow modeled tracer fields to reach near steady-state conditions.

Our goal here is to use these simulations to help bracket the Mediterranean Sea's uptake of anthropogenic CO_2 as well as its net transport across the Strait of Gibralter, while exploring how this marginal sea's heightened total alkalinity affects anthropogenic CO_2 uptake and corresponding changes in pH.

2 Methods

Anthropogenic CO_2 simulations were made offline with circulation fields from the NEMO circulation model. The same approach was used to make simulations of CFC-12 in order to evaluate modeled circulation, which heavily influences penetration of both of these passive transient tracers.

2.1 Circulation model

The regional circulation model NEMO-MED12 (Beuvier et al., 2012a) is a Mediterranean configuration of the free-surface ocean general circulation model NEMO (Madec and The-NEMO-Team, 2008). Its domain includes the whole Mediterranean Sea and extends into the Atlantic Ocean to 11°W; it does not include the Black Sea (Fig. 2). The horizontal model resolution is around 7 km, adequate to resolve key mesoscale features. Details of the model and its parametrizations are given by Beuvier et al. (2012a). NEMO-MED12 has been used to study the WMDW formation (Beuvier et al., 2012a), the response of the mixed layer to high-resolution ~~air–sea~~ air-sea forcings (Lebeaupin Brossier et al., 2011), and the transport across the Strait of Gibraltar (Soto-Navarro et al., 2014). NEMO-MED12 is descended from a suite of Mediterranean regional versions of OPA and NEMO used by the French modelling community: OPAMED16 (Béranger et al., 2005), OPAMED8 (Somot et al., 2006), NEMO-MED8 (Beuvier et al., 2010).

The physical simulation used here is very close to that described in Beuvier et al. (2012b). It is initiated in October 1958 with temperature and salinity data representative of the 1955–1965 period using the MEDATLAS dataset (MEDAR/MEDATLAS-Group 2002, Rixen et al., 2005).

For the Atlantic buffer, initial conditions are taken from the 2005 World Ocean Atlas for temperature (Locarnini et al., 2006) and salinity (Antonov et al., 2006). Boundary conditions are also needed to specify physical forcing for the atmosphere, freshwater inputs from rivers and the Black Sea, and exchange with the adjacent Atlantic Ocean. For the atmosphere, NEMO-MED12 is forced with daily evaporation, precipitation, radiative and turbulent heat fluxes, and momentum fluxes from the ARPERA dataset (Herrmann and Somot, 2008), all over the period 1958–2008. The ARPERA forcing constitutes a 56 year, high-resolution forcing (50 km, daily data) with a good temporal homogeneity (see Herrmann et al. (2010) for more details about the post-2001 period). The SST-relaxation and water-flux correction terms are applied as in Beuvier et al. (2012a). River runoff is derived by Beuvier et al. (2010, 2012a) from the interannual dataset of Ludwig et al. (2009) and Vörösmarty et al. (1996). Freshwater input from the Black Sea follows runoff estimates from Stanev and Peneva (2002). Exchange with the Atlantic is modelled through a buffer zone (see Fig. 2) between 11°W and the Strait of Gibraltar, where the model's 3-D temperature and salinity fields are relaxed to the observed climatology (Locarnini et al., 2006; Antonov et al., 2006) while superimposing anomalies of interannual variations from the ENSEMBLES reanalysis performed with a global version of NEMO (Daget et al., 2009). To reproduce the monthly cycle of the Mediterranean Sea's water volume, we restore the total sea-surface height (SSH) in the Atlantic buffer zone toward the monthly climatological values of the GLORYS1 reanalysis (Ferry et al., 2010)

The atmospheric forcing used by Beuvier et al. (2012b) does not include modifications to improve dense water fluxes through the Cretan Arc, which plays a critical role in deep-water formation during the Eastern Mediterranean Transient (EMT). As detailed by Roether et al. (1996, 2007), the EMT was a temporary change in the Eastern Mediterranean Deep Water (EMDW) formation that occurred when the source of this deep water switched from the Adriatic Sea to the Aegean Sea during 1992–1993. Beuvier et al. (2010) showed that a previous simulation with the circulation model NEMO-MED8 (1/8° horizontal resolution) was able to reproduce a transient in deep-water formation as observed for the EMT, but the simulated transient produced less EMDW. Beuvier et al. (2012b) later made a simulation with NEMO-MED12 with compariable forcing between October 1958 and December 2012. To improve the characteristics of the simu-

lated EMT, namely the density of newly formed EMDW during 1992–1993, its weak formation rate, and its shallow spreading at 1200 m, we made here a sensitivity test with modified forcing. For that, we modified the ARPERA forcings over the Aegean sub-basin, increasing mean values as done by Herrmann et al. (2008) to study the Gulf of Lions. More specifically, during November to March in the winters of 1991–1992 and 1992–1993, we increased daily surface heat loss by 40 $\mathrm{W\,m^{-2}}$, daily water loss by 1.5 $\mathrm{mm\,day^{-1}}$, and the daily wind stress modulus by 0.02 $\mathrm{N\,m^{-2}}$. That resulted in average wintertime increases in heat loss (+18 %), water loss (+41 %), and wind intensity (+17 %) over the Aegean sub-basin. The increased heat and water losses allow NEMO-MED12 to form denser water masses in the Aegean Sea during the most intense winters of the EMT, while increased wind stress drives more intense mixing via winter convection. Furthermore, enhanced convection accelerates the transfer of surface temperature and salinity perturbations into intermediate and deep layers of the Aegean Sea. In summary for this study, the physical model forcing is identical to that from Beuvier et al. (2012b), except for the enhanced forcing during the two winters mentioned above.

2.2 Passive tracer simulations

2.2.1 CFC-12

The trace atmospheric gas CFC-12 has no natural component. Being purely anthropogenic, its atmospheric concentration has increased since the 1930's and has leveled off in recent decades. Although sparingly soluble, it enters that ocean by gas exchange. There it remains chemically and biologically inert, tracking ocean circulation and mixing. Precise measurements of CFC-12 along several trans-Mediterranean sections make it particularly suited for evaluating these regional model simulations. To model CFC-12, we followed protocols from Phase 2 of the Ocean Carbon Cycle Model Intercomparison Project (OCMIP-2) as described by Dutay et al. (2002). For the air-to-sea flux of CFC-12 ($\mathrm{F_{CFC}}$), we used the standard formulation for a passive gaseous tracer

$$F_{\mathrm{CFC}} = k_{\mathrm{w}}(C_{\mathrm{eq}} - C_{\mathrm{surf}}) \quad (1)$$

where k_w is the gas transfer velocity (also known as the piston velocity), C_{surf} is the simulated sea-surface concentration of CFC-12, and C_{eq} is the atmospheric equilibrium concentration. That is,

$$C_{eq} = \alpha p\text{CFC} \tag{2}$$

where α is the CFC-12 solubility, a function of local seawater temperature and salinity (Warner and Weiss, 1985), and pCFC is the atmospheric partial pressure of CFC-12 computed from the atmospheric mole fraction in dry air. Here we assume atmospheric pressure remains at 1 atm neglecting spatiotemporal variations. The gas transfer velocity is computed from surface-level wind speeds (u) from the ARPERA forcing following the Wanninkhof (1992, Eq. 3) formulation

$$k_w = au^2 \left(\frac{Sc}{660}\right)^{-1/2} \tag{3}$$

where $a = 0.31$ and Sc is also the CFC-12 Schmidt number computed following Wanninkhof (1992, Table A1).

Regarding lateral boundary conditions, for the Atlantic buffer zone (between 11°W and Strait of Gibraltar), we assume that net exchange at the boundary may be neglected while relying on atmospheric exchange of this rapidly equilibrating tracer as the dominant factor.

2.2.2 Anthropogenic CO_2

To model anthropogenic CO_2 in the Mediterranean Sea, we use the perturbation approach (Siegenthaler and Joos, 1992; Sarmiento et al., 1992). This classic approach uses a simple relationship between the change in surface-ocean pCO_2, which is needed to compute the ~~air–sea~~ air-sea CO_2 flux, and the change in C_T. Such a relationship is necessary for carbon dioxide, unlike for CFC-12, because as CO_2 dissolves in the ocean it does not simply remain as a dissolved gas; it dissociates into two other inorganic species, bicarbonate and carbonate ions. When modeling only the change in the total of the three species (δC_T), the simple relationship that is used allows models to carry only that perturbation tracer.

In the perturbation approach, the geochemical driver is the atmospheric change in carbon dioxide. As written by Sarmiento et al. (1992), that change in terms of the partial pressure of carbon dioxide in moist air is

$$\delta p\mathrm{CO}_{2_\mathrm{a}} = (p\mathrm{CO}_{2_\mathrm{a}} - p\mathrm{CO}_{2_\mathrm{a},0})\,(1 - e_\mathrm{s}/p_\mathrm{a}) \tag{4}$$

For the model simulation, the two $p\mathrm{CO}_2$ terms (in $\mu\mathrm{atm}$) on the right side of the equation are identical to $x\mathrm{CO}_2$ (in ppm), although units differ, because they both refer to dry air and because the perturbation approach assumes a total atmospheric pressure of 1 atm. Of those two terms, $p\mathrm{CO}_{2_\mathrm{a},0}$ is the preindustrial reference value of $280\,\mu\mathrm{atm}$ (i.e., $x\mathrm{CO}_2 = 280\,\mathrm{ppm}$) and $p\mathrm{CO}_{2_\mathrm{a}}$ is the prescribed atmospheric $x\mathrm{CO}_2$ obtained from a spline fit to observations from the Siple ice core data and atmospheric CO_2 measurements from Mauna Loa, which together span 1800.0 to 1990.0 (Enting et al., 1994), combined with the 12 month smoothed Manua Loa atmospheric measurements between 1990.5 to 2009.0 (GLOBALVIEW-CO_2, 2010). The final term in Eq. (4) uses the saturation water vapor pressure e_s and the total atmospheric pressure at sea level p_a to convert partial pressure in dry air to that in wet air as needed to compute the ~~air–sea~~ air-sea flux.

The modeled ~~air–sea~~ air-sea flux of anthropogenic carbon F_{CO_2} follows the standard formulation

$$F_{\mathrm{CO}_2} = K_{\mathrm{CO}_2}(\delta p\mathrm{CO}_{2_\mathrm{a}} - \delta p\mathrm{CO}_{2_\mathrm{o}}) \tag{5}$$

where K_{CO_2} is a gas transfer coefficient, $\delta p\mathrm{CO}_{2_\mathrm{a}}$ is described above, and $\delta p\mathrm{CO}_{2_\mathrm{o}}$ is the anthropogenic perturbation in surface-water $p\mathrm{CO}_2$ relative to its reference value in 1800. For the gas transfer coefficient, $K_{\mathrm{CO}_2} = \alpha k_\mathrm{w}$, where α is the CO_2 solubility (Weiss, 1974) and $\mathrm{k_w}$ is as in Eq. (3) except that *Sc* is for CO_2 (Wanninkhof, 1992, Table A1).

The $\delta p\mathrm{CO}_{2_\mathrm{o}}$ term is not modeled explicitly but is calculated from the only tracer that is carried in the model, δC_T. The standard formulation from Sarmiento et al. (1992) is based on their finding that the relationship between the ratio $\delta p\mathrm{CO}_{2_\mathrm{o}}/\delta \mathrm{C_T}$ and $\delta p\mathrm{CO}_{2_\mathrm{o}}$ is linear, for

a given temperature and at constant total alkalinity.

$$\frac{\delta p\mathrm{CO}_{2_\mathrm{o}}}{\delta \mathrm{C_T}} = z_0 + z_1\,\delta p\mathrm{CO}_{2_\mathrm{o}} \tag{6}$$

where the intercept z_0 and slope z_1 terms are each quadratic functions of temperature. That equation is then rearranged for the model calculation.

$$\delta p\mathrm{CO}_{2_\mathrm{o}} = \frac{z_0\,\delta \mathrm{C_T}}{1 - z_1\,\delta \mathrm{C_T}} \tag{7}$$

To allow for a starting value of $p\mathrm{CO}_{2_{\mathrm{a},0}}$ that is different than 280 ppm, Lachkar et al. (2007) introduced two corrective terms

$$\delta p\mathrm{CO}_{2_\mathrm{o}} = \frac{z_0\,[\delta \mathrm{C_T} + \delta \mathrm{C_{T,corr}}]}{1 - z_1\,[\delta \mathrm{C_T} + \delta \mathrm{C_{T,corr}}]} - p\mathrm{CO}_{2_{\mathrm{a,corr}}} \tag{8}$$

where the first correction factor is

$$p\mathrm{CO}_{2_{\mathrm{a,corr}}} = p\mathrm{CO}_{2_{\mathrm{a},0}} - p\mathrm{CO}_{2_{\mathrm{a,ref}}} \tag{9}$$

determined from the starting $x\mathrm{CO}_2$ in the initial year (1800), i.e., $p\mathrm{CO}_{2_{\mathrm{a},0}} = 287.78$ ppm, and same reference $p\mathrm{CO}_{2_{\mathrm{a,ref}}} = 280$ ppm. With that result, the second correction factor is

$$\delta C_{\mathrm{T,corr}} = \frac{p\mathrm{CO}_{2_{\mathrm{a,corr}}}}{z_0 + z_1\,p\mathrm{CO}_{2_{\mathrm{a,corr}}}} \tag{10}$$

These two minor corrections do not change the way z_0 and z_1 are computed, but they do slightly alter their use in the model simulations, using Eq. (8) instead of Eq. (7).

Equations for the linear regression coefficients z_0 and z_1 are computed in four steps: (i) estimate the initial preindustrial $C_{\mathrm{T},0}$ as a function of temperature from carbonate system thermodynamics, assuming ~~air–sea~~ air-sea equilibrium between the atmosphere ($p\mathrm{CO}_{2_{\mathrm{a},0}} = 280$ ppm)

and the surface ocean, constant global-average surface total alkalinity ($2300\,\mu\mathrm{mol\,kg^{-1}}$), constant salinity ($35\,\mathrm{psu}$), and varying temperatures across the observed range; (ii) increase incrementally the $p\mathrm{CO}_{2_\mathrm{a}}$ from 280 to 480 ppm, and recompute the C_T as a function of temperature for each increment; (iii) use those results with Eq. (6) to compute z_0 and z_1 for each temperature; and (iv) fit each of z_0 and z_1 to a quadratic function of temperature. With this approach, Sarmiento et al. (1992) found that Eq. (6) fit exactly calculated values to within 1 % when $\delta p\mathrm{CO}_{2_\mathrm{o}} \leq 200\,\mathrm{ppm}$.

The constant value of total alkalinity used in the standard perturbation approach detailed above is the area-weighted mean for the global ocean. That approach with Eq. (8), which we refer to as GLO, will produce biased results for the Mediterranean Sea whose average surface total alkalinity is 10 % greater. Thus we made a second simulation (MED), where z_0 and z_1 that were used with Eq. (8) were computed following the same 4-step procedure as above, except that we replaced the area-weighted surface average total alkalinity for the global ocean ($2300\,\mu\mathrm{mol\,kg^{-1}}$) with that for the Mediterranean Sea ($2530\,\mu\mathrm{mol\,kg^{-1}}$).

Finally, to test how variable total alkalinity may affect simulated results, we made a third simulation (VAR). The perturbation approach was designed for the global, open-ocean waters where total alkalinity varies relatively little, e.g., from 2243 to $2349\,\mu\mathrm{mol\,kg^{-1}}$ in the zonal mean of the GLODAP gridded data product (Key et al., 2004). Spatial variations of surface total alkalinity in the Mediterranean Sea are more than twice as large, e.g., varying from 2375 to $2625\,\mu\mathrm{mol\,kg^{-1}}$ between western and eastern margins. To account for variability in Mediterranean total alkalinity, we exploited its tight relationship with salinity derived from the METEOR M51/2 transbasin section by Schneider et al. (2007)

$$A_\mathrm{T} = 73.7\,S - 285.7 \tag{11}$$

where S is the model's surface salinity and A_T is its computed surface total alkalinity. This equation thus takes much of the A_T spatial variablity into account (Fig. 3), although it is expected to be inaccurate near river mouths, where fresh waters with high total alkalinity are delivered to the Mediterranean Sea. This equation also implies that computed A_T varies temporally with simulated salinity.

For VAR to take into account variable salinity (total alkalinity) as well as variable temperature, while maintaining adequate precision, we made 2 types of modifications to the standard equations. First, we replaced Eq. (6) with a direct relationship between $\delta pCO_{2,o}$ and δC_T but with a cubic formulation instead of a linear formulation, i.e., implying an additional coefficient.

$$\delta pCO_{2,o} = 0 + z_1\,\delta C_T + z_2\,\delta C_T^2 + z_3\,\delta C_T^3 \tag{12}$$

Then for each of three coefficients, we replaced the former two equations, quadratic in temperature T, with three equations, cubic in T and S.

$$\begin{aligned} z_1 &= a_0 + a_1\,T + a_2\,S + a_3\,T^2 + a_4\,S^2 + a_5\,T^3 + a_6\,S^3 + a_7\,T\,S + a_8\,T^2\,S + a_9\,T\,S^2 \\ z_2 &= b_0 + b_1\,T + b_2\,S + b_3\,T^2 + b_4\,S^2 + b_5\,T^3 + b_6\,S^3 + b_7\,T\,S + b_8\,T^2\,S + b_9\,T\,S^2 \\ z_3 &= c_0 + c_1\,T + c_2\,S + c_3\,T^2 + c_4\,S^2 + c_5\,T^3 + c_6\,S^3 + c_7\,T\,S + c_8\,T^2\,S + c_9\,T\,S^2 \end{aligned} \tag{13}$$

The associated coefficients are listed in Table 7, while the R program used to make these calculations, which exploits the seacarb software package for the carbonate system (Lavigne and Gattuso, 2011), is given in the Supplement. With the VAR approach applied to the range of Mediterranean temperatures (13 to 30 °C) we found that Eq. (12) fit ~~exactly~~ calculated values to within 0.6 % when $\delta pCO_{2_a} \leq 280\,\mathrm{ppm}$, i.e., up to a doubling of the preindustrial level of atmospheric CO_2. Hence the simulated anthropgenic carbon is sensitive to the spatial and temporal changes in T in the GLO and MED experiments and T and S in the VAR experiment (Eq. (12)).

For lateral boundary conditions, we restored simulated δC_T throughout the Atlantic buffer zone toward a time varying, spatially co-located section taken from the global-scale gridded derived product by Khatiwala et al. (2009) for each year between 1765 to 2011, using their values from 1800 (the start year of our anthropogenic CO_2 simulations) as our zero reference. That damping across the entire buffer zone was designed to maintain a reasonable time varying inflow of δC_T from the Atlantic across the Strait of Gibraltar.

2.3 Looping

~~All numerical simulations were run~~ For computational efficiency, our geochemical simulations were made "off-line~~, looping through the circulation fields from~~". That is, they were driven by circulation fields that were read in from output from a previous simulation with the NEMO-MED12 ~~model. That circulation model was forced with the ARPERA~~ circulation model, thereby avoiding the need for us to recalculate them for each passive tracer simulation. Thus those circulation fields were computed by forcing the NEMO-MED12 with the APERA forcing during 1958–2008. We then looped repeatedly that 51-year sequence of model-circulation fields in order to cover the full 200-year industrial period for anthropogenic carbon simulations. The first 7 years of the circulation model (1958–1964) are considered as a spin-up and are not used in the offline simulations of passive tracers. ~~Rather, the~~ The next 10 years (ARPERA forcing during 1965–1974) are continuously repeated until 1975 to drive offline simulations of both passive tracers.

For both passive tracers, up until 1975, we began by looping repeatedly the same 10 years of NEMO-MED12 circulation fields, i.e., those forced by the ARPERA atmospheric forcing during 1965–1974. That forcing period was selected because it does not include intense events like the EMT or the Western Mediterranean Transition (Schroeder et al., 2008); we thus considered this period as best suited to produce reasonable circulation fields for the Mediterranean Sea (Beuvier et al., 2010, 2012b; Beuvier, 2011). Thus for the complete CFC-12 simulation, covering 1930 to 2008, the 1965–1974 loop of MED12 circulation fields was repeated 4.5 times to cover offline years 1930–1975~~(Fig. ??)~~. Then to complete the offline CFC-12 simulation, we applied the NEMO-MED12 circulation fields corresponding to the remaining 1975–2008 period forcing. The same 1965–1974 loop of the circulation fields from NEMO-MED12 were likewise repeated for the three anthropogenic CO_2 simulations (GLO, MED, VAR), but 17.5 times to cover offline simulation years 1800–1974. Then as for CFC-12, the last 34 years of the offline anthropogenic CO_2 simulations were piloted with the NEMO-MED12 circulation fields from the remaining 1975–2008 years of the ARPERA forcing.

2.4 δpH

The anthropogenic change in surface in situ pH during 1800 to 2001 was computed from δC_{T} and prescribed total alkalinity. The preindustrial C_{T} was computed by assuming ~~that~~ it to be in thermodynamic equilibrium with the prescribed total alkalinity ~~was in thermodynamic equilibrium~~ and with an atmospheric $x\mathrm{CO}_2$ of 280 ppm at 1 atm total pressure, correcting for humidity. Computations were made with seacarb, which takes two carbonate system variables and computes all others including pH. Then to this preindustrial C_{T}, we added our simulated δC_{T} and recomputed pH. Other input variables, temperature, salinity, and total alkalinity were identical. Concentrations of phosphate and silica were assumed to be zero, a good approximation for the oligotrophic surface waters of the Mediterranean Sea. The anthropogenic change in pH is then just the difference between two computations. This exercise yields a surface map of δpH.

For deep waters, we consider changes only along one transbasin section, Meteor M51/2. Exploiting total alkalinity, C_{T}, temperature, and salinity measured along from this section in November 2001 (Schneider et al., 2007, 2010), we computed corresponding pH for all data points along the section and throughout the water column. Then we subsampled the simulated δC_{T} in 2001 at all station locations and sample depths. After removing those simulated results from the measured C_{T}, we recalculated pH. The difference is the δpH along the same section. For comparison, we repeated this exercise, but instead of simulated δC_{T}, we used the TTD data-based estimates of anthropogenic C_{T} from Schneider et al. (2010), already available along the same section.

3 Results

3.1 Evaluation

By comparing modeled to observed CFC-12, we evaluated the simulated circulation in regard to ventilation of water masses (Fig. 4). Whereas modeled CFC-12 generally matches observations

between 150 m ($\sim$1.4 pmol kg^{-1}) and 1200 m ($\sim$0.3 pmol kg^{-1}), simulated concentrations do not show the observed mid-depth minimum. For instance in the Levantine sub-basin, observed CFC-12 concentrations are lowest ($\sim$ 0.3 pmol kg^{-1}) between 600 and 1500 m but below that depth zone concentrations grow with depth, reaching $\sim$0.6 pmol kg^{-1} in bottom waters. Conversely, simulated concentrations below 1200 m continue to decline until they bottom out at $\sim$0.3 pmol kg^{-1} (Fig. 5).

Generally, the model underestimates the relatively large CFC-12 concentrations observed in deep waters of the eastern and western basins ($\sim$0.6 pmol kg^{-1}), which are indicative of recently ventilated water masses (Schneider et al., 2010; Roether et al., 2007). Although the model simulates some penetration of CFC-12 south of the Crete Passage with concentrations reaching up to $\sim$0.5 pmol kg^{-1}, those remain lower than observed. Ventilation of the model's deep eastern basin is particularly weak in the Adriatic and Ionian sub-basins (Fig. 4). On average below 2000 m, CFC-12 concentration from the model are only half of those observed. Overall, the CFC-12 evaluation indicates that the model produces an adequate ventilation of intermediate water masses but insufficient ventilation of deep waters.

3.2 Air-sea flux

The invasion of anthropogenic carbon into the Mediterranean Sea is influenced by the δCO_2 flux at the surface and by exchange with the Atlantic Ocean across the Strait of Gibraltar. The simulated ~~air–sea flux~~ air-sea flux of anthropogenic carbon is calculated directly by the model (Eq. (5)). When integrated since the beginning of the simulation (cumulative flux)~~is~~ , it is found to be similar among the three simulations, all ~~exhibiting~~ of which exhibit maxima in the same regions (Fig. 6). The highest fluxes occur in the Gulf of Lions and to the east of Crete, both regions of deep and intermediate water formation, and in Alboran sub-basin, which is highly influenced by the strong Atlantic inflow and by the presence of 2 standing anticyclonic eddies (Vargas-Yáñez et al., 2002). Along coastlines there are local minima but also the maximum uptake at the outflow of the Dardanelles Strait although that is extremely localilzed. In the MED simulation, cumulative fluxes over the western basin are on average 25 % larger per unit area than the Mediterranean Sea's mean, whereas they are 13 % lower in the eastern basin (Table 1).

Conversely, the larger surface area of the eastern basin means that its total uptake represents 58 % of the total Mediterranean Sea uptake.

The 10 % greater prescribed surface total alkalinity in the MED simulation relative to GLO means that the latter must absorb less anthropogenic carbon (Fig. 6b). Indeed, despite very similar uptake patterns, the basin-wide cumulative uptake is 17 % less in the GLO simulation than in MED, with a greater reduction in the western basin (22 %) than in the eastern basin (14 %). By definition, the salinity-derived total alkalinity in the VAR simulation is more realistic than with MED simulation, varying from 2350 µeq kg^{-1} in the Alboran sub-basin to 2650 µeq kg^{-1} in the eastern basin. That lower western total alkalinity results in an 8 % lower ~~air–sea~~ air-sea flux in the western basin, while the higher eastern total alkalinity drives 5 % greater uptake in the eastern basin (Fig. 6c). Yet despite these east-west differences between VAR and MED, total basin-wide uptake is only 0.3 % less in former than the latter. Overall the eastern basin always dominates, taking up 60 % of the basin-wide integrated flux in VAR and GLO and taking up 57 % in MED. However, it is not only the ~~air–sea~~ air-sea flux but also lateral exchange that matters.

3.3 Budget

The Mediterranean Sea's content of anthropogenic carbon is affected not only by the ~~air–sea~~ air-sea flux but also by exchange with the Atlantic Ocean through the Strait of Gibraltar. To assess the relative importance of this lateral exchange we constructed a budget of δC_{T} in the Mediterranean Sea. In that, the temporal evolution of the cumulative ~~air–sea~~ air-sea flux in the reference simulation MED is compared to the same simulation's total mass of carbon that has entered and left the Mediterranean Sea through the Strait of Gibraltar (Fig. 7). The key terms are thus the flux, the net transfer at the Strait of Gibraltar (inflow – outflow of δC_{T}), and the actual accumulation of δC_{T} in the Mediterranean Sea (inventory).

In the MED simulation between 1800 and 2001, there is 1.50 Pg C that enters the Mediterranean Sea via the ~~air–sea~~ air-sea flux (0.78 Pg C) and via the Strait of Gibraltar inflow (0.72 Pg C) (Table 2). Yet 64 % of the δC_{T} inflow (by Atlantic Water near the surface) is balanced by δC_{T} outflow at depth (by the Mediterranean outflow). That leaves 1.04 Pg C that re-

mains in the Mediterranean as the total δC_{T} inventory. Thus 25 % of the Mediterranean's total δC_{T} inventory is due to net exchange at the Strait of Gibraltar, while the remaining 75 % is from the ~~air–sea~~ air-sea flux. The budget of the VAR simulation is quite similar to that for MED, but both of those differ substantially from the budget for GLO (Table 2). In GLO, the Mediterranean Sea's δC_{T} inventory in 2001 (0.94 Pg C) is 10 % less, with 69 % of the total input coming from the ~~air–sea~~ air-sea flux and 31 % from net exchange across the Strait of Gibraltar. The evolution of the MED simulation's carbon budget (Fig. 8) demonstrates that anthropogenic carbon enters the Mediterranean entirely via the ~~air–sea~~ air-sea flux at the beginning of the simulation, but that the fraction entering by lateral exchange across the Strait of Gibraltar grows until stabilizing in the 1960's to one-fourth of the total.

3.4 Simulated δC_{T} inventory

Having examined how anthropogenic carbon enters the Mediterranean Sea, we now turn to where it is stored, the patterns of which differ from those of the input fluxes due to water mass transport. The vertical integral of the δC_{T} concentration is termed the inventory. In the Mediterranean Sea, the inventory patterns tend to follow the distribution of bathymetry (Fig. 9). Thus unlike the global ocean, substantial levels of anthropogenic carbon have already penetrated into deep waters of the Mediterranean Sea, as deduced previously by observational studies (Lee et al., 2011; Schneider et al., 2010; Touratier and Goyet, 2011). Specific inventories (mass per unit area) in the reference simulation (MED) are 10 % higher in the western basin and 6 % lower in the eastern basin relative to the 33.5 $\mathrm{mol\,C\,m^{-2}}$ average for the Mediterranean Sea (Table 3). For the two other simulations, the basin-wide inventory is 10 % lower in GLO and 0.1 % higher in VAR. Those east-west differences are smaller than those for the ~~air–sea~~ air-sea flux (Table 1). There is a strong correlation between latitudinal variations in the inventory and the bathymetry, both along the METEOR M51/2 section and in terms of meridional means (Fig. 10). In both cases, the correlation is striking, except in isolated regions such as in the Ionian sub-basin ($\sim$15–20°E in Fig. 10) where poorly ventilated deep waters have relatively low δC_{T} concentrations.

3.5 Comparison with TTD data-based ~~estimates~~results

To go beyond model comparison of simulated uptake of anthropogenic CO_2, we also compare model results to data-based estimates. In particular, we focused on data-based estimates of anthropogenic carbon deduced with TTD because that method requires only measurements of temperature, salinity, and CFC-12, all of which were simulated thereby allowing us to test the approach (see Sect. 4.1). For now though, let us simply compare model results to the TTD ~~data-based~~ estimates of δC_{T} ~~estimated from~~ based on observations collected on the METEOR M51/2 section in 2001 (Schneider et al., 2010). A first comparison reveals that the ~~model underestimates everywhere the TTD data-based~~ modeled δC_{T} is everywhere lower than the TTD estimates of the inventory along the METEOR M51/2 section (Fig. 9). While the TTD inventory along this section averages 83 $\mathrm{mol\,m^{-2}}$ (ranging from 21 and 153 $\mathrm{mol\,m^{-2}}$), the model average is 50 $\mathrm{mol\,m^{-2}}$, 40 % less. Expanding the comparison vertically, the model δC_{T} is seen to underestimate the ~~data-based estimates~~ TTD results throughout the water column, even at the surface (Fig. 11). Surface concentrations are naturally largest, both for the TTD estimates ($\sim$68 $\mu\mathrm{mol\,kg^{-1}}$) and for the model (e.g., $\sim$58 $\mu\mathrm{mol\,kg^{-1}}$ in the MED simulation). Whereas the TTD ~~data-based~~ estimates are lowest (20 to 25 $\mu\mathrm{mol\,kg^{-1}}$) in the Levantine sub-basin between 800 and 1500 m and increase below (e.g., reaching up to 35 $\mu\mathrm{mol\,kg^{-1}}$ in the EMDW), simulated δC_{T} decreases with depth everywhere, as already seen for simulated CFC-12 (Fig. 4). The lowest simulated δC_{T} concentrations are found in the bottom waters of the Ionian sub-basin ($< 5\,\mu\mathrm{mol\,kg^{-1}}$). However, higher deep-water δC_{T} is simulated in the EMDW near the Crete Passage (up to 15 $\mu\mathrm{mol\,kg^{-1}}$), where there is dense-water outflow from the Aegean sub-basin through the Crete Passage, during the EMT. In terms of basin totals, Schneider et al. (2010) relied on TTD to help estimate a basin-wide anthropogenic carbon inventory of 1.7 Pg C for the Mediterranean Sea, with 1.0 Pg C of that in the Eastern basin (Table 4). Relative to the data-based ~~estimates~~TTD results, the modeled basin-wide Mediterranean inventory is 40 % less in the MED and VAR and 46 % less in GLO. For the eastern inventory basin, the MED and VAR simulations are 35 % lower than the TTD ~~data-based~~ estimates, whereas GLO is 42 % lower.

3.6 δpH

Anthropogenic changes in surface pH between 1800 and 2001 are remarkably uniform, both between simulations and across the basin. Away from the coast, the change in surface pH between 1800 and 2001 varies between ~~-0.078~~ -0.082 and ~~-0.082~~ -0.086 in the GLO simulation (Fig. 12). Exceptions include the Northern Levantine sub-basin, where the δpH is slightly less ~~intense~~ ~~(-0.076)and the more intense changes~~ -0.080), and the greater changes seen in the Gulf of Gabes, the Adriatic and Aegean sub-basins, ~~and~~ as well as near the mouths of large rivers such as the Nile and the Rhone. The MED simulation exhibits almost identical patterns and intensities for the change in pH except in Alboran sub-basin and the western portion of the Western basin, where pH changes are less intense ($-$~~0.074~~ -0.076 and $-$~~0.072~~-0.074, i.e., a difference of up to ~~~ 0.008~~ ~ 0.012 pH units). Conversely, the VAR simulation with its spatially varying total alkalinity produces a more contrasted pattern of pH change. Although VAR 's spatial variability in δpH in the western basin is intermediate between that seen for GLO and MED, the eastern basin contrast in VAR is much greater. In particular, VAR 's pH changes are smallest where the salinity derived total alkalinity is highest (Levantine sub-basin), and they are largest where the salinity-derived total alkalinity is smallest (e.g., near the Po, Nile, and Dardanelles outflows). Despite differences in spatial patterns between simulations, their basin-wide average change in surface pH is almost identical ~~-0.08 ± 0.01~~ -0.084 ± 0.001 units (total scale).

4 Discussion

4.1 δC_{T} in the Mediterranean Sea

Our comparison of modeled to measured CFC-12 indicates that the model adequately represents ventilation of near-surface and intermediate waters but underestimates ventilation of deep waters. This CFC-12 evaluation alone implies that our simulated δC_{T} is likewise too low in Mediterranean Sea deep waters and hence that our simulated total anthropogenic carbon inventory of 1.03 Pg C is a lower limit. Yet even in the top 400 m where there is tight agreement be-

tween simulated and observed CFC-12, the data-based estimates of δC_{T} from the TTD method are 20 % larger than those simulated (Fig. 5). Hence it is unlikely that the modeled circulation is the primary cause. Simplifications with the perturbation approach, e.g., its steady state assumption, could be partly to blame although errors due to circulation-induced changes in biological productivity appear small for the global ocean (Siegenthaler and Sarmiento, 1993; Sarmiento et al., 1998). Nor does the treatment of total alkalinity in the perturbation approach appear a significant factor, considering that our three treatments with different mean states and spatial variability give results that are quite similar (see Sect. 4.3). Besides these potential simulation biases, it is also possible that the data-based methodology, namely the TTD approach, is biased.

Hence we tested the TTD approach in the model world (MW) by (1) using exactly the same version and parametrizations of the TTD approach that described in Schneider et al. (2010) for consistency; (2) using it to estimate δC_{T} from simulated CFC-12, temperature, and salinity and (23) comparing those results to the δC_{T} simulated directly by the model. That comparison reveals that the $\mathrm{TTD_{MW}}$ estimates always overestimate the simulated δC_{T}. Those overestimates start at $+10\,\%$ in surface waters but reach more than $+100\,\%$ in Mediterranean Sea bottom waters (Fig. 13). Relative differences are highest where simulated CFC-12 is lowest, i.e., where the ventilation age of water masses are oldest, namely in bottom waters particularly those in the Ionian sub-basin. Whereas the $\mathrm{TTD_{MW}}$ estimate of the total anthropogenic carbon inventory in the Mediterranean Sea is $1.4\,\mathrm{Pg\,C}$, the simulated value in the reference simulation (MED) is $1.0\,\mathrm{Pg\,C}$. That 40 % overestimate with the TTD approach in the model world could be less in the real Mediterranean Sea, because the model underestimates CFC-12 concentrations in the deep water, which accentuates the discrepancy. Nonetheless, the TTD-based inventory of anthropogenic carbon remains an upper limit.

One reason for this overestimate is that data-based methods such as TTD assume that the change in oceanic pCO_2 is identical to the change in the atmospheric pCO_2. This convenient assumption, that $\Delta\delta pCO_2 = 0$, has been motivated by measured pCO_2 at 3 time-series (BATS, HOT, and ESTOC), where calculated atmospheric and oceanic trends are not significantly different (Bindoff et al., 2007) . However, these stations are all located in subtropical gyres where both the air-sea flux of anthropogenic CO_2 and the corresponding

air-sea disequilibrium are the lowest (Figure 2 in Sarmiento et al. (1992)), i.e, where the detection of an air-sea disequilibrium in temporal changes of pCO_2 (i.e., $\Delta\delta pCO_2$) is the most difficult. Our model estimates estimations of this disequilibrium in the Mediterranean Sea (Fig. 14) indicate that it is not negligible. It slowly increases from 1800 up to 14 to 20 μatm in 2001, corresponding to a lag of ocean's δpCO_2 compared to the atmosphere's by 15 to 20% since $\sim$1850. These $\Delta\delta pCO_2$ values are similar to those simulated by global ocean models (Sarmiento et al., 1992; **?**; Yool et al., 2010) . Assuming that this disequilibrium is zero, as done in TTD, implies a systematic overestimate of anthropogenic carbon uptake.

Other data-based methods that estimate greater anthropogenic carbon inventories than TTD in the Mediterranean Sea, e.g., the TrOCA approach (Fig. 1), must overestimate the true inventory by even more. Although even the upper limit of our range (1.0 to 1.7 $\mathrm{Pg\,C}$) is small when compared to the global ocean inventory of anthropogenic carbon of 134 $\mathrm{Pg\,C}$ (Sabine et al., 2004, for year 1994), the Mediterranean Sea contains 2.4 to 4 times as much anthropogenic carbon per unit volume as does the global ocean.

4.2 Transfer across the Strait of Gibraltar

Unlike the global ocean where outside input of anthropogenic carbon comes only from the atmosphere, in the Mediterranean Sea there is also lateral input and output of anthropogenic carbon via the Strait of Gibraltar. Unfortunately, data-based estimates of that net transport do not agree even in terms of its direction, much less its magnitude. That is, estimates of transport based on data-based estimates of δC_{T} with the TrOCA method suggest that the Mediterranean Sea is a source anthropogenic carbon to the Atlantic Ocean (Aït-Ameur and Goyet, 2006; Huertas et al., 2009); conversely, with two other data-based methods, TTD and the ΔC^* approach (Gruber et al., 1996), there is a net transport of anthropogenic carbon from the Atlantic to the Mediterranean Sea (Huertas et al., 2009; Schneider et al., 2010). The two latter back-calculation data-based methods give similar net fluxes of δC_{T}: $\sim$4.2 $\mathrm{Tg\,C\,yr^{-1}}$ with ΔC^* and 3.5 $\mathrm{Tg\,C\,yr^{-1}}$ with TTD. Both rely on the estimates of water fluxes from Huertas et al. (2009) (Table 5). Both methods also produce similar estimates for the δC_{T} concentrations in inflowing and outflowing waters: $\sim$60 $\mu\mathrm{mol\,kg^{-1}}$ in the near-surface inflowing water and $\sim$52 $\mu\mathrm{mol\,kg^{-1}}$

in the deeper Mediterranean Outflow Water (MOW). However, these δC_{T} estimates are based on data collected from different periods, i.e., May 2005 to July 2007 for Huertas et al. (2009) and November 2001 for Schneider et al. (2010). Moreover, the transfer deduced from TTD-derived δC_{T} estimates from Schneider et al. are estimated to have a large uncertainty (-1.8 to $9.2\,\mathrm{Tg\,C\,yr^{-1}}$). The net δC_{T} transfer estimated with the TrOCA method is $-3\,\mathrm{Tg\,C\,yr^{-1}}$. That much stronger net export from the Mediterranean Sea to the Atlantic is due to TrOCA's assessment that the outflowing MOW has higher δC_{T} ($\sim$80 $\mu\mathrm{mol\,kg^{-1}}$) than the inflowing AW ($\sim$65 $\mu\mathrm{mol\,kg^{-1}}$) (Huertas et al., 2009; Schneider et al., 2010; Flecha et al., 2011). Yet that vertical distribution is opposite to that expected from an anthropogenic transient tracer in the ocean with an atmospheric origin.

All three of our model simulations indicate a net transfer of anthropogenic carbon from the Atlantic to the Mediterranean across the Strait of Gibraltar (Sect. 3.3). In the reference simulation (MED), 0.26 Pg C enters the Mediterranean Sea via the Strait fo Gibralter between 1800 and 2001, similar to the TTD- and ΔC^*-based estimates (Table 5). Observational estimates of water transfer across the Strait of Gibraltar are between 0.72 and 1.01 Sv (1 Sverdrup (Sv) $= 10^6\,\mathrm{m^3\,s^{-1}}$) for surface inflow and between 0.68 and 0.97 Sv for deep outflow, resulting in a net transfer of $+0.04$ to $+0.13$ Sv (Bryden and Kinder, 1991; Bryden et al., 1994; Tsimplis and Bryden, 2000; Candela, 2001; Baschek et al., 2001; Lafuente et al., 2002; Soto-Navarro et al., 2010). The model falls near the lower limit of these estimates, having an inflow of 0.71 Sv, an outflow of 0.67 Sv, and a net water transfer of $+0.04$ Sv, when averaged between 1992 to 2008 (Beuvier, 2011). For 2005–2007, the simulated transfer is 0.15 Sv weaker than observational estimates from Huertas et al. in 2001 both for inflow and outflow, while net transfer is not significantly different: $+0.04$ vs. 0.05 Sv (Table 5).

Simulated δC_{T} concentrations in the model's AW are largely determined by damping to data-based estimates from Khatiwala et al. (2009) at the western boundary of the model domain. In the MED simulation, the δC_{T} in the inflowing AW is 12 to 24 % lower than data-based estimates from Huertas et al. (2009) who used both ΔC^* and TrOCA approaches (Table 5). But the largest discrepancy occurs in the outflowing deeper waters (MOW), for which the simulated δC_{T} underestimates the data-based ΔC^* for 2005–2007 by 31 %. That underestimate is

expected given that simulated CFC-12 in the model's WMDW is only half that observed and that this deep water contributes to the MOW.

The model's underestimate of δC_{T} in the MOW is the determining factor which results in less outflow and thus more net inflow of anthropogenic carbon to the Mediterranean Sea. It follows that the model must provide an upper limit for the true net inflow of anthropogenic carbon, given that modeled water exchange falls within the observed range and that modeled and data-based estimates of δC_{T} are more similar in the inflowing water than in the outflowing water. Likewise, a lower limit for net transport of anthropogenic is offered by the computations that use data-based TTD estimates of δC_{T}. That follows because (1) TTD overestimates deep δC_{T} by more than surface values and (2) near surface inflow and deep outflow are similar in magnitude. Hence the TTD-based approach must underestimate net input of anthropogenic carbon to the Mediterranean. Therefore the net input of anthropogenic carbon across the Strait of Gibralter must be between $+3.5$ and $+4.7\,\mathrm{Tg\,C\,yr^{-1}}$ based on observations collected in 2001. To compare that range to the Huertas et al.'s results for 2005–2007, we relied on the simulated δC_{T} evolution between 2001 and 2005–2007. In that 5 ± 1 year period, simulated δC_{T} increased by $+10.5\,\%$ in the inflowing AW and by $+11.2\,\%$ in the MOW. For the 2005–2007 lower limit, we applied those trends to the lower limit δC_{T} estimates for 2001 (Schneider et al.'s TTD estimates in the AW and MOW) combined with the 2005–2007 water transfer rates (Huertas et al., 2009); for the upper limit we again used the model result. Hence for 2005–2007, we consider that the true net input of anthropogenic carbon across the Strait of Gibraltar must fall between $+3.7$ and $+5.5\,\mathrm{Tg\,C\,yr^{-1}}$.

4.3 Sensitivity to total alkalinity

To test the sensitivity of results to total alkalinity we compared three simulations: GLO with a basin-wide total alkalinity equal to the global ocean average, MED where the basin-wide inventory is increased by $10\,\%$ (equivalent to the Mediterranean Sea's surface average), and VAR where surface total alkalinity varies as a linear function of salinity. The $10\,\%$ greater total alkalinity in MED and VAR relative to GLO results in a $10\,\%$ greater simulated inventory of anthropogenic carbon (Table 4), but the basin-integrated ~~air–sea~~ air-sea flux of anthropogenic

in MED and VAR is 20 % greater than in GLO (Table 1). The 10 % difference must be made up by proportionally less input of anthropogenic carbon to the Mediterranean from the Atlantic in MED and VAR relative to GLO.

The MED simulation has greater total alkalinity in the western basin than either GLO or VAR and hence it absorbs more anthropogenic carbon there than do the other two simulations (Fig. 6). Yet MED 's western basin total alkalinity is too high compared to what actually comes in from the Atlantic and even in terms of the δC_{T} also coming in with the same water. The latter is determined in all three model runs by restoring to data-based estimates of Khatiwala et al. (2009) in the Atlantic buffer zone. Thus it is less accurate to impose a mean Mediterranean Sea total alkalinity in this area, which artificially increases the surface water buffer capacity and hence its ability to absorb CO_2. The same artefact results in a lower local change in pH (Fig. 12). Thus the constant Mediterranean surface total alkalinity as used in MED is suboptimal for simulating δC_{T} near the Strait of Gibraltar.

In contrast, the VAR simulation generally has more realistic total alkalinity that increases from west to east (Fig. 3). That avoids an over-buffered carbonate system near the Strait of Gibraltar, particularly in the Alboran sub-basin, and an under-buffered system in the far eastern Mediterranean. However, VAR is generally less realistic near river mouths than either GLO or MED. By imposing a total alkalinity that is a function of salinity in a model that considers only fresh water riverine input (no total alkalinity delivery), the model-imposed total alkalinity near river mouths is too low. That artefact results in lower air-to-sea fluxes of anthropogenic carbon when close to river mouths (Fig. 6) and locally more intense reductions in pH near the Nile, Po, and Rhone river mouths and near the outflow of the Dardanelles Strait (Fig. 12); at the latter site, the air-to-sea flux of anthropogenic carbon even changes sign from ocean uptake to loss, although that is extremely localized.

Despite these local differences, the three approaches yield similar results when integrated across the entire Mediterranean Sea, with spatial variability in total alkalinity leading to differences in global inventory of only 0.1 % and differences between east-west partitioning of less than 1 %.

4.4 Change in pH

Two recent studies have attempted to quantify the decline in the pH of the Mediterranean Sea due to the increase in anthropogenic carbon (Touratier and Goyet, 2009, 2011). Both concluded that the pH reduction in the Mediterranean Sea (acidification), is larger than that experienced by typical waters of the global ocean. The higher total alkalinity of the Mediterranean Sea was evoked to justify a larger uptake of anthropogenic carbon. Our results support that finding, i.e., with the MED – GLO showing a 10 % increase in anthropogenic carbon inventory that occurs when average surface total alkalinity is increased by 10 % (Mediterranean minus global ocean average).

The same two studies further suggest that higher levels of δC_{T} in the Mediterranean Sea also imply greater changes in pH. Yet our sensitivity tests demonstrate that the higher total alkalinity of the Mediterranean Sea does not result in a greater anthropogenic reduction in surface pH. Differences between simulations GLO and MED are negligible (Fig. 12). In both, the simulated decline in surface pH is ~~−0.08~~ 0.084 ±0.001 units when averaged across Mediterranean Sea (Table 6). Hence the decline in pH is quite similar between typical surface waters in the Mediterranean Sea and those in the global ocean. Furthermore, because it is on a log scale, absolute differences in pH actually represent relative changes in $[H^+]$. To avoid such confusion, we prefer to discuss acidification of the Mediterranean Sea in terms of $[H^+]$.

~~For clearer illustration, let us compare these findings from an ocean model, where oceanic and atmospheric are not in equilibrium, with calculations that assume thermodynamic equilibrium. By imposing the same atmospheric increase (from 280 to 450) to be in equilibrium with surface water at three different alkalinities (2300, 2450 and 2600), we can for each total alkalinity compute corresponding changes in all other carbonate system variables, including C_{T} and pH~~ For a quantitative understanding of how total alkalinity affects surface acidification, we made additional equilibrium calculations to assess rates of change in terms of $\partial C_T / \partial \mathrm{pCO_2}$ and $\partial[H^+]/\partial \mathrm{pCO_2}$ (Fig. 15).

~~At the beginning (280~~Those were computed from analytical expressions for buffer factors (Egleston et al., 2010) , corrected and rearranged as by Orr (2011) . Both quantities change over

the range of across the observed west-east gradient of the Mediterranean's surface alkalinity (2380 to 2650), the higher total alkalinity produces higher calculated C_T and higher calculated pH. At each total alkalinity, as atmospheric increases, calculated C_T increases and calculated pH decreases. The same change in atmospheric from 280 to 450μ produces larger changes in calculated C_T when total alkalinity is larger (e.g. , a 14greater increase with a total alkalinity of 2600 instead of 2300mol) . Conversely, corresponding changes in pH differ by less than 1. This simple equilibrium calculation confirms our ocean model results as well as results from a previous study (Orr, 2011, Fig. 3.6) . Although the higher total alkalinity of the Mediterranean Sea enhances its anthropogenic carbon content by 10, kg^{-1}), when temperature and salinity held their western, minimum value.

The equilibrium experiment on Mediterranean C_T change rate confirms our sensitivity test results: that the west-to-east increase in alkalinity alone increases ∂C_T /∂pCO_2 by 12%(Fig 15b), corresponding to the equivalent west-to-east change in anthropogenic C_T (Fig 15d). Let see what happen in the case of the acidification rate (Fig 15a). The west-to-east increase in alkalinity alone reduces $\partial[H^+]/\partial pCO_2$ by 8%. Then after including the west-to-east temperature increase (6°C during summer) the anthropogenic reduction in surface pH is not significantly different from that for typical surface waters of the global ocean$\partial[H^+]/\partial pCO_2$ is reduced by another 0.5% (i.e., for the east relative to the west). But the temperature reduction in $\partial[H^+]/\partial pCO_2$ is compensated by the west-to-east increase in salinity (3 units on the practical salinity scale) during summer. For comparison, there is a 2% decrease in $\partial[H^+]/\partial pCO_2$ as atmospheric xCO_2 increases from 280 to 385 ppm and another 4% decrease when atmospheric xCO_2 increases further to 850 ppm. The resulting west-to-east difference in $[H^+]$ changes globally correspond to a decrease of -10.5% between 1765 and 2008 (Fig 15c). These equilibrium calculations highlight the alkalinity effect on Mediterranean anthropogenic acidification. It confirms higher δC_T uptake, and a lower $[H^+]$ decrease due to its higher alkalinity.

The model's surface acidification rates (Fig. 16 are slightly less intense, because it does not make the simplification that atmospheric and oceanic pCO_2 are identical (i.e., in equilibrium). The acidification rate is 8% lower in MED (~17.5 pmol kg^{-1} μatm^{-1} in 2001) than in GLO

(∼19.1 pmol kg^{-1} μatm^{-1} in 2001). In VAR, the ∂[H$^+$]/∂pCO$_2$ decreases by 8% in 2001 when moving from west to east (from ∼18.5 to ∼17 pmol kg^{-1} μatm^{-1}). That modeled west-to-east gradient is much like that found with the thermodynamic calculations, but curves are displaced downwards by 0.3 units.

Anthropogenic carbon is already present in substantial quantities throughout the water column of the Mediterranean Sea (Fig. 11). Hence the anthropogenic decline in pH also affects the entire water column. Touratier and Goyet (2011) found that the anthropogenic pH change in some Mediterranean bottom waters has already reached values of up to −0.12, higher even than at the surface. However, they deduce those high values from data-based estimates of δC_{T} using the TrOCA approach, which overestimates actual values, particularly at depth (see Sects. 1 and 4.1). To estimate subsurface anthropogenic changes in pH, we used a simple 3-step method: (1) we relied on discrete measurements of C_{T}, total alkalinity, and phosphate and silicate concentrations on the 2001 Meteor M51/2 cruise to compute a modern reference pH using seacarb; (2) we subsampled the MED model at the same time, positions, and depths to get corresponding simulated δC_{T}; and (3) we subtracted the latter from the modern measurements of C_{T} to get preindustrial C_{T}, using that along with the measured values of other input variables (assuming they had not changed) to compute a preindustrial pH. We then compared that model-derived change in pH (δpH$_{\mathrm{model}}$) to the data-based TTD estimates (δpH$_{\mathrm{TTD}}$) calculated in the same fashion, i.e., using TTD δC_{T} instead of modeled δC_{T} in the computation sequence (Fig. 17). The resulting anthropogenic change in surface pH ranges from −0.08 to −0.10 units. Below the surface, δpH$_{\mathrm{model}}$ gradually becomes less intense until reaching the bottom where it ranges from −0.005 pH units in the Ionian sub-basin to −0.03 in the Crete Passage. Those changes must be underestimates given the model's poor ventilation of deep waters based on the CFC-12 evaluation (Sect. 3.1). The data-based change in δpH$_{\mathrm{TTD}}$ exhibits its weakest magnitude (−0.035 pH units) between 1000 and 1500 m in the Levantine sub-basin, where the TTD data-based δC_{T} is at a minimum. Deeper down, δpH$_{\mathrm{TTD}}$ increases in magnitude, reaching up to −0.06 pH units in the bottom waters of the Ionian sub-basin.

As the model results and the TTD data-based approach provide lower and upper limits for the actual changes in deep-water δC_{T}, it follows that they also provide bounds for the anthropogenic

change in pH. The actual change in bottom water pH in the eastern basin thus lies between -0.005 and -0.06 units.

5 Conclusions

A first simulation of anthropogenic carbon in the Mediterranean Sea suggests that it accumulated $1.0\,\mathrm{Pg\,C}$ between 1800 and 2001. That estimate provides a lower limit based on comparison of observed vs. simulated CFC-12 in the same model, which reveals that modeled deep waters are poorly ventilated compare to observations. Furthermore, we demonstrate that a previous data-based estimate of $1.7\,\mathrm{Pg\,C}$ (Schneider et al., 2010) is an upper limit after testing the associated TTD approach in our model. In 2001 in the reference model, a total of $1.5\,\mathrm{Pg\,C}$ of anthropogenic carbon had entered the Mediterranean Sea with 52 % from the ~~air–sea~~ air-sea flux and 48 % from Atlantic Water inflow; however, 31 % of that total had also left via the deep Mediterranean Outflow Water. Out of the net accumulation of $1.0\,\mathrm{Pg\,C}$, 75 % comes from the air-to-sea flux and 25 % from net transfer across the Strait of Gibraltar. The rate of net exchange across that strait to the Mediterranean is from 3.5 to $4.7\,\mathrm{Tg\,C\,yr^{-1}}$ in 2001 and from 3.7 to $5.5\,\mathrm{Tg\,C\,yr^{-1}}$ in 2005–2007, based on the model and TTD results.

Our estimates of anthropogenic carbon also allow us to assess anthropogenic changes in pH. Although the 10 % higher mean total alkalinity of the Mediterranean Sea is responsible for a 10 % increase in anthropogenic carbon inventory, that does not significantly affect the anthropogenic change in surface pH. That average surface pH change -0.08 units for both the Mediterranean Sea and the global ocean. In contrast, relative to the global ocean, Mediterranean deep waters exhibit a larger anthropopogenic change in pH because their ventilation times are faster. In 2001, the δpH in Mediterranean Sea bottom waters is estimated to lie between -0.005 to -0.06 units based on our limits from simulated and TTD data-based δC_{T}. These findings do not support previous conclusions that the anthropogenic change in the pH of Mediterranean deep waters is as high as -0.12 units, which is more intense even than the surface change (Touratier and Goyet, 2009, 2011). Furthermore those previous findings rely on the TrOCA

data-based estimates of δC_{T}, which are much larger than the TTD data-based estimates, shown in Sect. 4.1 to be already an upper limit.

Future studies that include the full natural carbon cycle and the effects of climate change are needed to confirm these results and predict future changes while weighing geochemical vs. climate factors. Improved assessment of local changes along coastlines will require improved boundary conditions, particularly for riverine and groundwater discharge of nutrients, carbon, and total alkalinity, combined with developments to improve coastal aspects of the physical and biogeochemical models.

The Supplement related to this article is available online at doi:10.5194/bgd-0-1-2014-supplement.

Acknowledgements. We thank Samar Khatiwala for providing his data-based estimates for anthropogenic carbon, which we used as a lateral boundary condition for the Atlantic portion of our model domain. We thank Météo-France/CNRM and in particular Michel Déqué and Florence Sevault for running and providing the ARPERA dataset. We also thank Marte Álvarez and an anonymous referee for their insightful reviews, which have helped to improve this manuscript. This work was supported by the French SiMED project (Mercator Ocean), the MORCE and MED-ICCBIO projects (GIS), and the EU FP7 project MedSeA (grant 265103). This work is a contribution to the HyMeX and MERMEX programmes, and it was granted access to the HPC resources of IDRIS (Institut du Développement et des Ressources en Informatique Scientifique) of the Centre National de la Recherche Scientifique (CNRS) under allocations for years 2010, 2011 and 2012 (project 1010227) made by Grand Equipement National de Calcul Intensif (GENCI).

References

Aït-Ameur, N. and Goyet, C.: Distribution and transport of natural and anthropogenic CO_2 in the Gulf of Cádiz, Deep-Sea Res. Pt. II, 53, 1329–1343, 2006.

Álvarez, M., Sanleón-Bartolomé, H., Tanhua, T., Mintrop, L., Luchetta, A.,Cantoni, C., Schroeder, K., Civitarese, G.: The CO_2 system in the Mediterranean Sea: a basin wide perspective, Ocean Science, 10, 69–92, 2014, doi:10.5194/os-10-69-2014

Antonov, J. I., Locarnini, R. A., Boyer, T. P., Mishonov, A. V., and Garcia, H. E.: World Ocean Atlas 2005, vol. 2: Salinity, edited by: Levitus, S., NOAA Atlas NESDIS 62, US Government Printing Office, Washington DC, 182 pp., 2006.

Attané, I. and Courbage, Y.: La démographie en Méditerranée, Situation et projections, Economica – Plan Bleu, 2001.

Attané, I. and Courbage, Y.: Demography in the Mediterranean region: situation and projections, Plan Bleu, 2004.

Baschek, B., Send, U., Lafuente, J. G., and Candela, J.: Transport estimates in the Strait of Gibraltar with a tidal inverse model, J. Geophys. Res., 106, 31033–31, 2001.

Béranger, K., Mortier, L., and Crépon, M.: Seasonal variability of water transport through the Straits of Gibraltar, Sicily and Corsica, derived from a high-resolution model of the Mediterranean circulation, Prog. Oceanogr., 66, 341–364, 2005.

Beuvier, J.: Modélisation de la variabilité climatique et des masses d'eau en mer Méditerranée: impact des échanges océan-atmosphère, Ph. D. thesis, Ecole Polytechnique, Palaiseau, France, 2011.

Beuvier, J., Sevault, F., Herrmann, M., Kontoyiannis, H., Ludwig, W., Rixen, M., Stanev, E., Béranger, K., and Somot, S.: Modelling the Mediterranean Sea interannual variability over the last 40 years: focus on the EMT, J. Geophys. Res., 115, C08017, doi:10.1029/2009JC005950, 2010.

Beuvier, J., Béranger, K., Lebeaupin Brossier, C., Somot, S., Sevault, F., Drillet, Y., Bourdallé-Badie, R., Ferry, N., and Lyard, F.: Spreading of the Western Mediterranean Deep Water after winter 2005: Time scales and deep cyclone transport, J. Geophys. Res., 117, C07022 doi:10.1029/2011JC007679, 2012a.

Beuvier, J., Lebeaupin Brossier, C., Béranger, K., Arsouze, T., Bourdallé-Badie, R., Deltel, C., Drillet, Y., Drobinski, P., Lyard, F., Ferry, N., Sevault, F., and Somot, S.: MED12, Oceanic component for the modelling of the regional Mediterranean Earth System, Mercator Ocean Quarterly Newsletter, 46, 60–66, 2012b.

Bindoff, N. L., Willebrand, J., Artale, V., Cazenave, A., Gregory, J. M., Gulev, S., Hanawa, K., Le Quéré, C., Levitus, S., Nojiri, Y., Shum, C. K., Talley, L. D., and Unnikrishnan, A. S.: Observations: Oceanic climate change and sea level, in Climate Change 2007: The Physical Science Basis. Contribution of Working Group I to the Fourth Assessment Report of the Intergovern- mental Panel on Climate Change, edited by S. Solomon et al., chap. 5, Cambridge University Press, Cambridge, United Kingdom and New York, NY.

Bryden, H. L. and Kinder, T. H.: Steady two-layer exchange through the Strait of Gibraltar, Deep-Sea Res. Pt. I, 38, S445–S463, 1991.

Bryden, H. L., Candela, J., and Kinder, T. H.: Exchange through the Strait of Gibraltar, Prog. Oceanogr., 33, 201–248, 1994.

Candela, J.: Mediterranean Water and Global Circulation, vol. 77, Elsevier, 419 pp., 2001.

Daget, N., Weaver, A., and Balmaseda, M.: Ensemble estimation of background-error variances in a three-dimensional variational data assimilation system for the global ocean, Q. J. Roy. Meteor. Soc., 135, 1071–1094, 2009.

Diffenbaugh, N. S. and Giorgi, F.: Climate change hotspots in the CMIP5 global climate model ensemble, Climatic Change, 114, 813–822, 2012.

Dutay, J.-C., Bullister, J. L., Doney, S. C., Orr, J. C., Najjar, R., Caldeira, K., Campin, J.-M., Drange, H., Follows, M., Gao, Y., Gruber, N., Hecht, M. W., Ishida, A., Joos, F., Lindsay, K., Madec, G., Maier-Reimer, E., Marshall, J. C., Matear, R. J., Monfray, P., Mouchet, A., Plattner, G.-K., Sarmiento, J., Schlitzer, R., Slater, R., Totterdell, I. J., Weirig, M.-F., Yamanaka, Y. and Yool, A.: Evaluation of ocean model ventilation with CFC-11: comparison of 13 global ocean models, Ocean Model., 4, 89–120, 2002.

Egleston, E. S., Sabine, C. L., and Morel, F. M. M.: Revelle revisited: Buffer factors that quantify the response of ocean chemistry to changes in DIC and alkalinity, Global Biogeochem. Cycles, 24, GB1002, doi:10.1029/2008GB003407

El Boukary, M. M. S.: Impact des activités humaines sur les cycles biogéochimiques en mer Méditerranée, Ph. D. thesis, Unniversité Paris VI - Pierre et Marie Curie, 2005.

Enting, I. G., Wigley, T. M. L., and Heimann, M.: Future emissions and concentrations of carbon dioxide: key ocean/atmosphere/land analyses, Tech. pap. 31, Div. of Atmos. Res., Commonw. Sci., and Ind. Res. Org., Melbourne, Australia, 1994.

Ferry, N., Parent, L., Garric, G., Barnier, B., Jourdain, N. C., and the Mercator-Ocean-team: Mercator global eddy permitting ocean reanalysis GLORYS1V1: description and results, Merc. Oc. Quart. Newsletter, 36, 15–28, 2010.

Flecha, S., Pérez, F. F., Navarro, G., Ruiz, J., Olivé, I., Rodríguez-Gálvez, S., Costas, E., and Huertas, I. E.: Anthropogenic carbon inventory in the Gulf of Cádiz, J. Marine Syst., 92, 67–75, 2011.

Gibelin, A.-L., and Déqué, M.: Anthropogenic climate change over the Mediterranean region simulated by a global variable resolution model, Clim. Dynam., 20, 327–339, 2003.

Giorgi, F.: Climate change hot-spots, Geophys. Res. Lett., 33, L08707, doi:10.1029/2006GL025734, 2006.

Giorgi, F. and Lionello, P.: Climate change projections for the Mediterranean region, Glob. Planet. Change, 63, 90–104, doi:10.1016/j.gloplacha.2007.09.005, 2008.

GLOBALVIEW–CO_2: Cooperative Atmospheric Data Integration Project – Carbon Dioxide, NOAA ESRL, Boulder, Colorado, available at: http://www.esrl.noaa.gov/gmd/ccgg/globalview, 2010.

Gruber, N., Sarmiento, J. L., and Stocker, T. F.: An improved method to detect anthropogenic CO_2 in the oceans., Global Biogeochem. Cy., 10, 809–837, 1996.

Herrmann, M. and Somot, S.: Relevance of ERA40 dynamical downscaling for modeling deep convection in the Mediterranean Sea, Geophys. Res. Lett., 35, L04607, doi:10.1029/2007GL032442, 2008.

Herrmann, M., Somot, S., Sevault, F., Estournel, C., and Déqué, M.: Modeling the deep convection in the northwestern Mediterranean Sea using an eddy-permitting and an eddy-resolving model: Case study of winter 1986–1987, J. Geophys. Res., 113, C04011, doi:10.1029/2006JC003991, 2008.

Herrmann, M., Sevault, F., Beuvier, J., and Somot, S.: What induced the exceptional 2005 convection event in the Northwestern Mediterranean basin? Answers from a modeling study., J. Geophys. Res., 115, C12051, doi:10.1029/2010JC006162, 2010.

Huertas, I. E., Ríos, A. F., García-Lafuente, J., Makaoui, A., Rodríguez-Gálvez, S., Sánchez-Román, A., Orbi, A., Ruíz, J., and Pérez, F. F.: Anthropogenic and natural CO_2 exchange through the Strait of Gibraltar, Biogeosciences, 6, 647–662, doi:10.5194/bg-6-647-2009, 2009.

Key, R. M., Sabine., C. L., Lee, K., Wanninkhof, R., Bullister, J., Feely, R. A., Millero, F. J., Mordy, C., and Peng, T.-H.: A global ocean carbon climatology: results from Global Data Analysis Project (GLODAP), Global Biogeochem. Cy., 18, GB4031, doi:10.1029/2004GB002247, 2004.

Khatiwala, S., Primeau, F., and Hall, T.: Reconstruction of the history of anthropogenic CO_2 concentrations in the ocean, Nature, 462, 346–349, doi:10.1038/nature08526, 2009.

Lachkar, Z., Orr, J. C., Dutay, J.-C., and Delecluse, P.: Effects of mesoscale eddies on global ocean distributions of CFC-11, CO_2, and $\Delta^{14}C$, Ocean Sci., 3, 461–482, doi:10.5194/os-3-461-2007, 2007.

Lafuente, J. G., Delgado, J., Vargas, J. M., Vargas, M., Plaza, F., and Sarhan, T.: Low-frequency variability of the exchanged flows through the Strait of Gibraltar during CANIGO, Deep-Sea Res. Pt. II, 49, 4051–4067, 2002.

Lavigne, H. and Gattuso, J.-P.: seacarb: seawater carbonate chemistry with R. R package version 2.4, available at: http://CRAN.R-project.org/package=seacarb, 2011.

Lebeaupin Brossier, C., Béranger, K., Deltel, C., and Drobinski, P.: The Mediterranean response to different space-time resolution atmospheric forcings using perpetual mode sensitivity simulations, Ocean Model., 36, 1–25, doi:10.1016/j.ocemod.2010.10.008, 2011.

Lee, K., Sabine, C. L., Tanhua, T., Kim, T.-W., Feely, R. A., and Kim, H.-C.: Roles of marginal seas in absorbing and storing fossil fuel CO_2, Energy Environ. Sci., 4, 1133–1146, doi:10.1039/C0EE00663G, 2011.

Locarnini, R. A., Mishonov, A. V., Antonov, J. I., Boyer, T. P., and Garcia, H. E.: World Ocean Atlas 2005, Volume 1: Temperature, S. Levitus, Ed., NOAA Atlas NESDIS 61, US Government Printing Office, Washington, D. C., 182 pp., 2006.

Ludwig, W., Dumont, E., Meybeck, M., and Heussner, S.: River discharges of water and nutrients to the Mediterranean and Black Sea: Major drivers for ecosystem changes during past and future decades?, Prog. Oceanogr., 80, 199–217, doi:10.1016/j.pocean.2009.02.001, 2009.

Madec, G. and The-NEMO-Team: NEMO ocean engine, Note du pole de modélisation de l'IPSL no. 27, Institut Pierre Simon Laplace, ISSN No. 1228–1619, 2008.

artOrr2001

Orr, J. C., Monfray, P., Maier-Reimer, E., Mikolajewicz, U., Palmer, J., Taylor, N. K., Toggweiler, J. R., Sarmiento, J. L., Le Quere, C., Gruber, N, Sabine, C. L., Key, R. M., and Boutin, J.: Estimates of anthropogenic carbon uptake from four threedimensionsal global ocean models, Global Biogeochem. Cycles, 15, 43–60, 2001.

Orr, J. C.: Recent and future changes in ocean carbonate chemistry, in: Ocean Acidification, edited by: Gattuso, J. and Hansson, L., Oxford University press, Oxford, 41–66, 2011.

Roether, W., Manca, B., Klein, B., Bregant, D., Georgopoulos, D., Beitzel, V., Kovacevic, V., and Luchetta, V.: Recent changes in eastern Mediterranean deep waters, Science, 271, 333–335, doi:10.1126/science.271.5247.333, 1996.

Roether, W., Klein, B., Manca, B. B., Theocharis, A., and Kioroglou, S.: Transient Eastern Mediterranean deep waters in response to the massive dense-water output of the Aegean Sea in the 1990s, Prog. Oceanogr., 74, 540–571, doi:10.1016/j.pocean.2007.03.001, 2007.

Sabine, C. L., Feely, R. A., Gruber, N., Key, R. M., Lee, K., Bullister, J. L., Wanninkhof, R., Wong, C. S., Wallace, D. W. R., Tilbrook, B., Millero, F. J., Peng, T.-H., Kozyr, A., Ono, T., and Rios, A.: The ocean sink for anthropogenic CO_2, Science, 305, 367–370, doi:10.1126/science.1097403, 2004.

Sarmiento, J. L., Orr, J. C., and Siegenthaler, U.: A perturbation simulation of uptake in an ocean general circulation model, J. Geophys. Res., 97, 3621–3645, 1992.

Sarmiento, J. L., Hughes, T. M., Stouffer, R. J., and Manabe, S.: Simulated response of the ocean carbon cycle to anthropogenic climate warming, Nature, 393, 245–249, 1998.

Schneider, A., Wallace, D. W. R., and Körtzinger, A.: Alkalinity of the Mediterranean Sea, Geophys. Res. Lett., 34, L15608, doi:10.1029/2006GL028842, 2007.

Schneider, A., Tanhua, T., Körtzinger, A., and Wallace, D. W. R.: High anthropogenic carbon content in the eastern Mediterranean, J. Geophys. Res., 115, C12050, doi:10.1029/2010JC006171, 2010.

Schroeder, K., Ribotti, A., Borghini, M., Sorgente, R., Perilli, A., and Gasparini, G.: An extensive western Mediterranean deep water renewal between 2004 and 2006, Geophys. Res. Lett., 35, L18605, doi:10.1029/2008GL035146, 2008.

Siegenthaler, U. and Joos, F.: Use of a simple model for studying oceanic tracer distributions and the global carbon cycle, Tellus B, 44, 186–207, 1992.

Siegenthaler, U. and Sarmiento, J.: Atmospheric carbon dioxide and the ocean, Nature, 365, 119–125, 1993.

Somot, S., Sevault, F., and Déqué, M.: Transient climate change scenario simulation of the Mediterranean Sea for the 21st century using a high-resolution ocean circulation model., Clim. Dynam., 27, 851–879, doi:10.1007/s00382-006-0167-z, 2006.

Soto-Navarro, J., Criado-Aldeanueva, F., García-Lafuente, J., and Sánchez-Román, A.: Estimation of the Atlantic inflow through the Strait of Gibraltar from climatological and in situ data, J. Geophys. Res., 115, C10023, doi:10.1029/2010JC006302, 2010.

Soto-Navarro, J., Somot, S., Sevault, F., Beuvier, J., Béranger, K., Criado-Aldeanueva, F., and García-Lafuente, J.: Evaluation of regional ocean circulation models for the Mediterranean Sea at the strait of Gibraltar: volume transport and thermohaline properties of the outflow, Clim. Dynam., in revision, 2014.

Stanev, E. V. and Peneva, L.: Regional sea level response to global climatic change: Black Sea examples, Global Planet. Change, 32, 33–47, 2002.

The MerMEX group: Marine ecosystems' responses to climatic and anthropogenic forcings in the Mediterranean, Prog. Oceanogr., 91, 97–166, doi:10.1016/j.pocean.2011.02.003, 2011.

Touratier, F. and Goyet, C.: Decadal evolution of anthropogenic CO_2 in the northwestern Mediterranean Sea from the mid-1990s to the mid-2000s, Deep-Sea Res. Pt. I, 56, 1708–1716, 2009.

Touratier, F. and Goyet, C.: Impact of the Eastern Mediterranean Transient on the distribution of anthropogenic CO_2 and first estimate of acidification for the Mediterranean Sea, Deep-Sea Res. Pt. I, 58, 1–15, doi:10.1016/j.dsr.2010.10.002, 2011.

Touratier, F., Azouzi, L., and Goyet, C.: CFC-11, $\delta^{14}C$ and ^{3}H tracers as a means to asses anthropogenic CO_2 concentrations in the ocean, Tellus B, 59, 318–325, 2007.

Tsimplis, M. and Bryden, H.: Estimation of the transports through the Strait of Gibraltar, Deep-Sea Res. Pt. I, 47, 2219–2242, 2000.

Vargas-Yáñez, M., Plaza, F., Garcıa-Lafuente, J., Sarhan, T., Vargas, J., and Velez-Belchi, P.: About the seasonal variability of the Alboran Sea circulation, J. Marine Syst., 35, 229–248, 2002.

Vörösmarty, C. J., Fekete, B. M., and Tucker, B. A.: Global River Discharge Database (RivDIS V1.0), International Hydrological Program, Global Hydrological Archive and Analysis Systems, UNESCO, Paris, 1996.

Wanninkhof, R.: Relationship between wind speed and gas exchange over the ocean, J. Geophys. Res., 97, 7373–7382, 1992.

Warner, M. J. and Weiss, R. F.: Solubilities of chlorofluorocarbons 11 and 12 in water and seawater, Deep-Sea Res. Pt. I, 32, 1485–1497, 1985.

Waugh, D. W., Hall, T. M., McNeil, B. I., Key, R., and Matear, R. J.: Anthropogenic CO_2 in the oceans estimated using transit time distributions, Tellus B., 58, 376–389, 2006.

Weiss, R. F.: Carbon dioxide in water and seawater: the solubility of a non-ideal gas, Mar. Chem., 2, 203–215, 1974.

Yool, A., Oschlies, A., Nurser, A. J. G., and Gruber, N : A model-based assessment of the TrOCA approach for estimating anthropogenic carbon in the ocean , Biogeosciences., 7, 2, 723–751, 2010.

Table 1. Cumulative flux between 1800 and 2001 for the three simulations, given in $\mathrm{mol\,C\,m^{-2}}$ and in Pg C for the Eastern and Western basins and for the entire Mediterranean Sea.

	Average flux ($\mathrm{mol\,C\,m^{-2}}$)			Total flux (Pg C)		
	East	West	Med Sea	East	West	Med Sea
GLO	19.2	24.8	21.0	0.39	0.26	0.65
MED	22.3	31.8	25.5	0.45	0.33	0.78
VAR	23.4	29.4	25.4	0.47	0.31	0.78

Table 2. Budget of the anthropogenic carbon accumulated in the Mediterranean Sea (Pg C) between 1800 and 2001. The budget distinguishes Strait of Gibralter inflow ($G - S_{\text{In}}$) via the AW, the corresponding outflow ($G - S_{\text{Out}}$) via the MOW, and the ~~air–sea~~ air-sea flux (~~air–sea~~air-sea). Critical combined terms are thus the net inflow-outflow difference (Net $G - S$), the Total Input ($G - S_{\text{In}}+$ ~~air–sea~~air-sea), and the Net Total (Net $G - S+$ ~~air–sea~~air-sea).

Simulation	$G - S_{\text{In}}$	$G - S_{\text{Out}}$	Net $G - S$	~~air–sea~~ air-sea	Total Input	Net Total
GLO	0.71	0.42	0.29	0.65	1.36	0.94
MED	0.72	0.46	0.26	0.78	1.5	1.04
VAR	0.72	0.46	0.26	0.78	1.5	1.04

Table 3. Average δC_{T} inventories (mol C m^{-2}) in the eastern and western basins and for the entire Mediterranean Sea.

	Average inventory (mol C m^{-2})		
Simulation	East	West	Med Sea
GLO	28.6	33.4	30.2
MED	31.8	36.9	33.5
VAR	32.0	36.6	33.6

Table 4. Total δC_{T} inventory (Pg C) for the entire Mediterranean Sea and for just the Eastern basin as simulated and as estimated by the TTD data-based method (Schneider et al., 2010).

Approach	Med Sea	East
GLO model	0.93	0.58
MED model	1.03	0.65
VAR model	1.03	0.65
TTD data	1.7 (1.3–2.1)	1.0 (0.7–1.2)

Table 5. Lateral fluxes of water and anthropogenic carbon across the Strait of Gibraltar.

Approach	Year(s)	Net fluxes[7] ($\mathrm{Tg\,C\,yr^{-1}}$)	Q_{in} (Sv)	$\delta C_{\mathrm{T;in}}$ ($\mu\mathrm{mol\,kg^{-1}}$)	Q_{out} (Sv)	$\delta C_{\mathrm{T;out}}$ ($\mu\mathrm{mol\,kg^{-1}}$)
$(\Delta C^*)^{1,2}$	2005–2007	$+4.20 \pm 0.04$	0.89	60	0.85	51
$(\Delta C^*)^{1,3}$	2005–2007		0.85	61	0.81	52
$(\mathrm{TrOCA})^{1,2}$	2005–2007	-3.00 ± 0.04	0.89	64	0.85	78
$(\mathrm{TrOCA})^{1,3}$	2005–2007		0.85	69	0.81	81
$(\mathrm{TTD})^{4}$	2001	$+3.5$ (-1.8 to 9.2)	0.89[5]	62.4[6]	0.85[5]	54.8
Model MED	2001	$+4.7$	0.70	47.6	0.66	32.1
Model MED	2005–2007	$+5.5$	0.74	52.6	0.69	35.7

[1] Huertas et al. (2009) estimates based on data near the Strait of Gibraltar during 2005–2007.
[2] method applied to observations on the Atlantic side of the Strait of Gibraltar.
[3] method applied to observations on the Mediterranean side of the Strait of Gibraltar during May 2005 to Jul 2007.
[4] Schneider et al. (2010) estimates using the TTD approach with observations from 2001.
[5] Schneider et al.'s water fluxes across the Strait of Gibralter are from Huertas et al. (2009).
[6] Schneider et al.'s δC_{T} concentration in inflowing AW is from Aït-Ameur and Goyet (2006).
[7] Positive values indicate transfer from the Atlantic to the Mediterranean Sea.

Table 6. Average changes in pH and [H^+] between 1800 and 2001 for the three simulations in the whole Mediterranean Sea and its western and eastern basins.

	δpH			$\delta[H^+]$ (nmol kg^{-1})		
	West	East	Med Sea	West	East	Med Sea
GLO	-0.0851	-0.0849	-0.0850	1.45	1.46	1.46
MED	-0.0823	-0.0848	-0.0840	1.29	1.35	1.33
VAR	-0.0833	-0.0837	-0.0836	1.33	1.32	1.32

Table 7. Coefficients a_i, b_i, and c_i (where the index i varies from 0 to 9) used to compute z_1, z_2, and z_3 with Eq. (13).

i	a_i	b_i	c_i
0	1.177825e+1	9.330105e−2	1.350359e−3
1	−1.614090e−1	−1.857070e−3	−2.422081e−5
2	−5.633789e−1	−5.251668e−3	−8.087972e−5
3	1.102070e−3	1.615968e−5	1.558226e−7
4	1.027733e−2	1.028834e−4	1.655765e−6
5	−4.195387e−6	−5.816404e−8	−3.503140e−10
6	−6.677595e−5	−6.915741e−7	−1.151323e−8
7	5.292828e−3	6.857606e−5	9.547726e−7
8	−1.529681e−5	−2.836387e−7	−3.012886e−9
9	−4.737909e−5	−6.551447e−7	−9.651931e−9

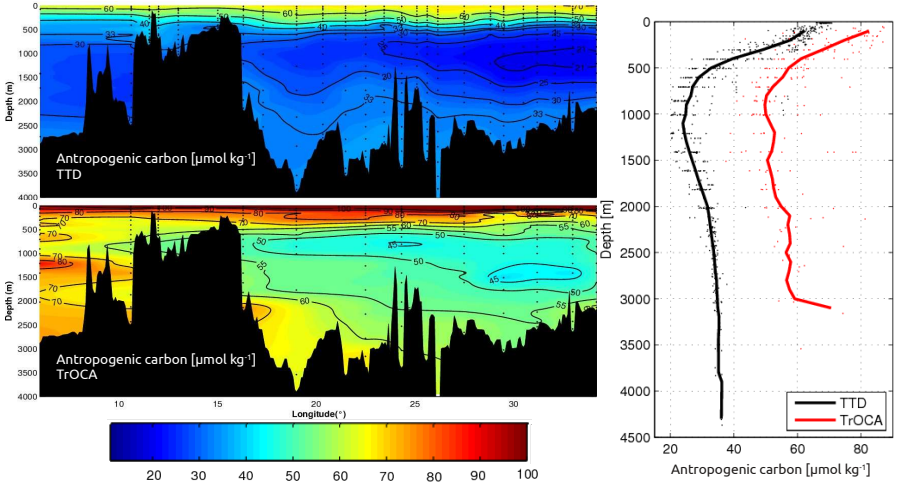

Figure 1. Anthropogenic carbon ($\mu\mathrm{mol\,kg^{-1}}$) estimated with two data-based methods, TTD (Schneider et al., 2010) and TrOCA (Touratier and Goyet, 2011), along the METEOR M51/2 section (November 2001). Vertical profiles on the right are for mean anthropogenic C_{T} along the section estimated by each method (Note that the vertical profile of the TrOCA method does not go below 3500m depth because it needs measurements some of which where not available at that depth).

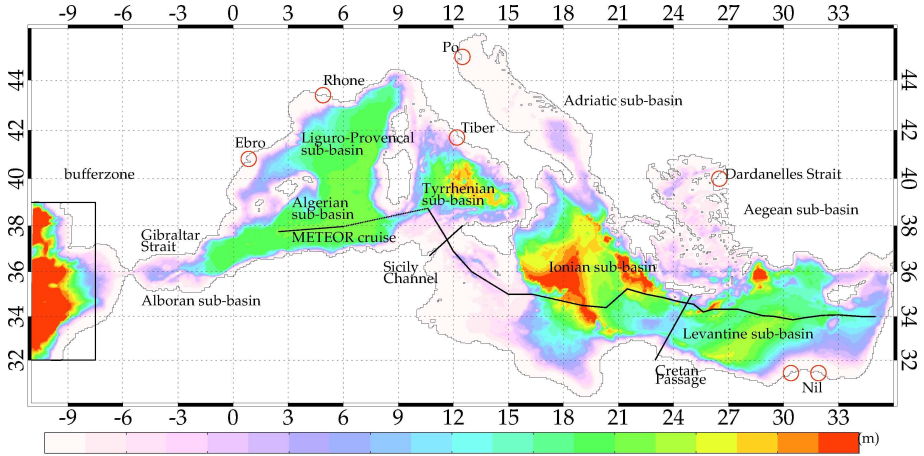

Figure 2. Map of the MED12 model domain and bathymetry with location of the main Mediterranean sub-basins (s-b): Adriatic, Aegean, Alboran, Algerian, Liguro-Provençal, Ionian, Levantine, and Tyrrhenian. Red circles indicate the mouths of the main Mediterranean rivers (Ebro, Rhone, Tiber, Po, and Nile) and the input from the Black Sea at the Dardanelles strait. Black lines indicate the Sicily channel, the Crete Passage, and the trans-Mediterranean section from the METEOR M51/2 cruise (november 2001). The rectangular area in the western part of the model domain indicates the Atlantic bufferzone (see Sects. 2.1 and 2.2.2). The eastern basin is situated to the east of the Sicily Channel, while the western basin is situated between the Strait of Gibraltar and the Sicily Channel. The entire Mediterranean Sea refers to all waters east of the Strait of Gibraltar.

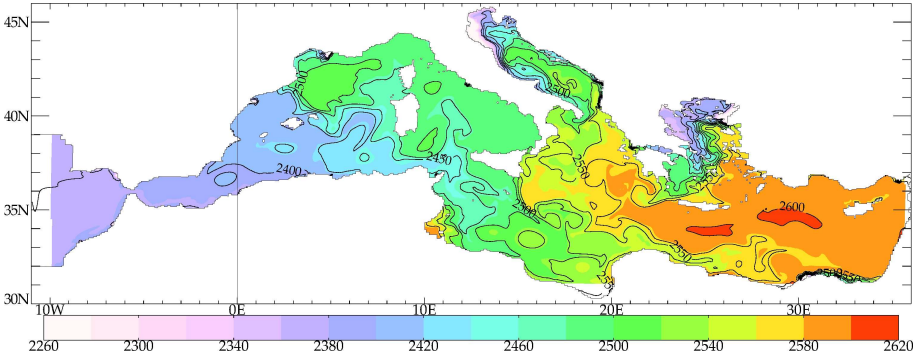

Figure 3. Salinity-derived surface total alkalinity field ($\mu\mathrm{mol\,kg^{-1}}$) calculated with Schneider et al.'s (2007) formula (Eq. 11) applied to the model's surface salinity field from November 2001.

~~Looping of dynamical atmospheric forcing fields for our CFC-12 and δC_{T} simulations. Colors indicate the year of the forcing.~~

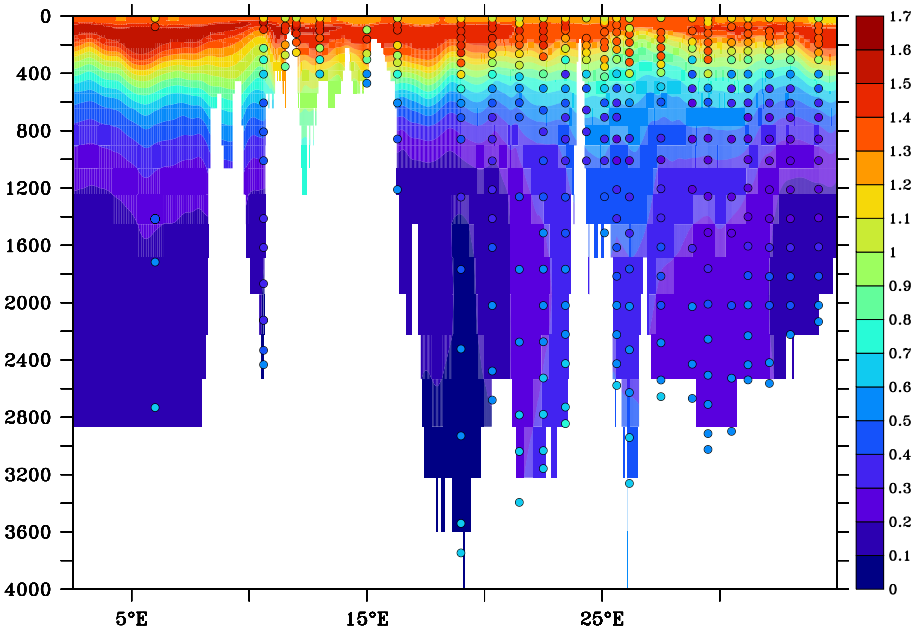

Figure 4. CFC-12 (pmol kg^{-1}) data-model comparison along the METEOR M51/2 section. Color-filled contours indicate simulated CFC-12, whereas color-filled dots show in-situ observations. Both use the same color scale and are taken at the same time (November 2001).

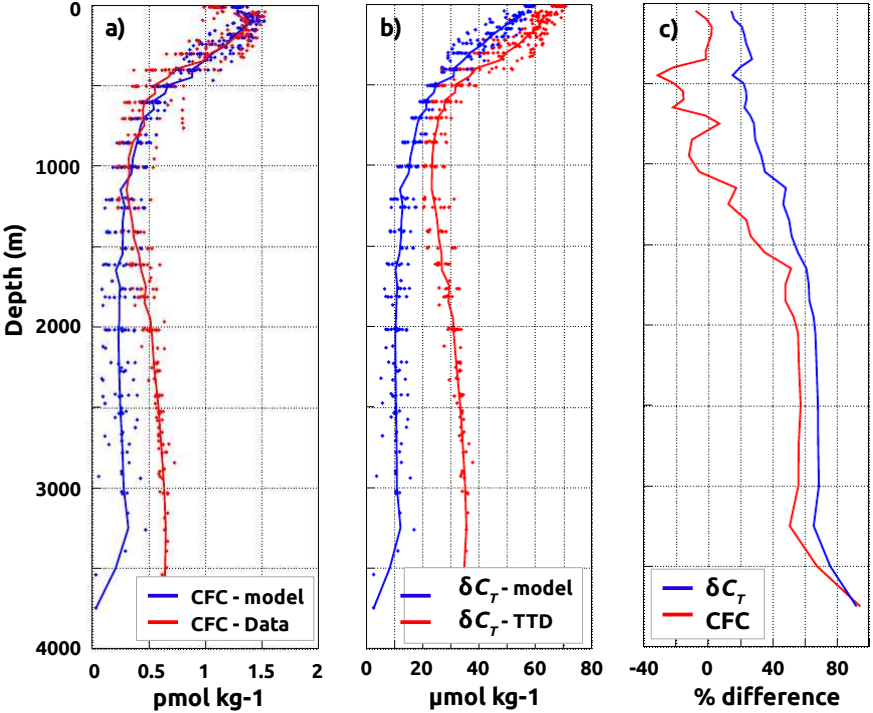

Figure 5. Comparison of average vertical profiles along the METEOR M51/2 section for **(a)** CFC-12 (pmol kg^{-1}), **(b)** δC_{T} (μmol kg^{-1}), and **(c)** the model-data relative difference (in percent). Model results are in blue, while red indicates the CFC-12 data and δC_{T} data-based estimates; the right panel **(c)** uses blue for δC_{T} and red for CFC-12. Data-based estimates for δC_{T} are the TTD results from Schneider et al. (2010).

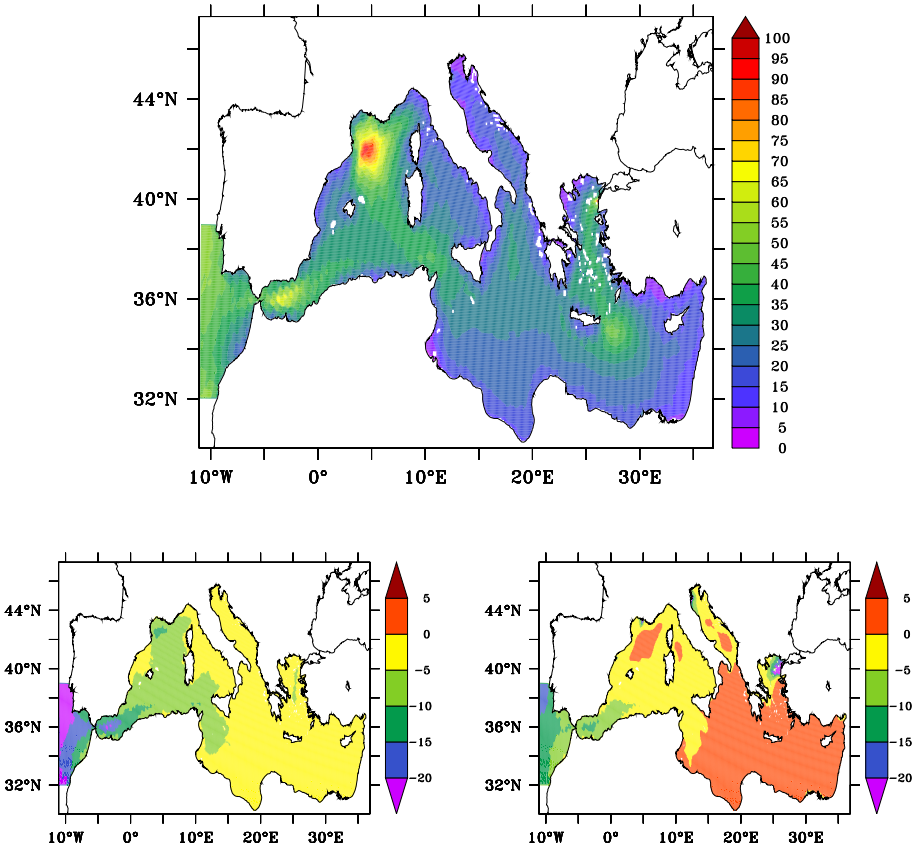

Figure 6. Cumulative air-to-sea flux of anthropogenic carbon (mol m^{-2}) from 1800 to November 2001 shown as the total flux for the MED reference simulation (top) and for the other two simulations as differences: GLO − MED (bottom left) and VAR − MED (bottom right).

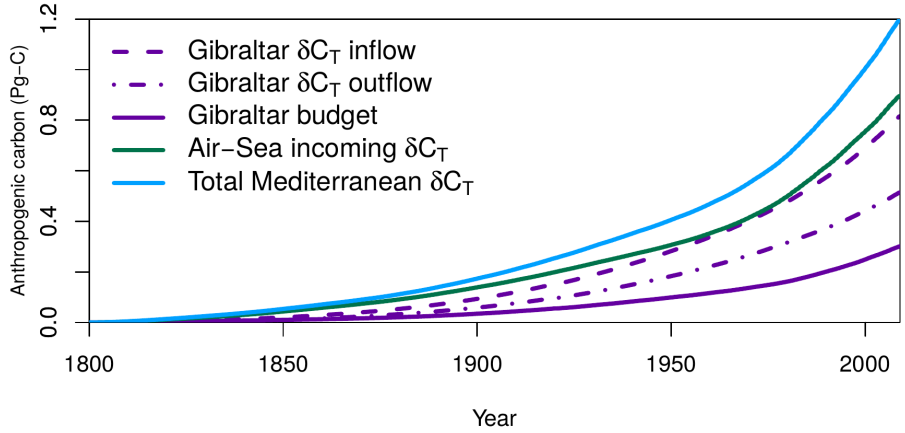

Figure 7. Cumulative increase in anthropogenic carbon (Pg C) in the Mediterranean Sea from 1800 to 2008 due to the Gibraltar inflow (~~large~~ dashed~~and dotted~~, purple) and outflow (dashed and dotted, purple), i.e., their difference (inflow − outflow, solid, purple) ~~,~~ and the ~~air−sea~~ air-sea flux (solid, green). Also shown is the total buildup in ~~inventory~~ storage (solid, light blue). Gibraltar fluxes have been calculated from model monthly mean outputs, by multiplying the anthropogenic carbon concentration ($g\,m^{-3}$) of water in a section crossing the Gibraltar strait, by by water fluxes ($m^3\,month{-}1$) flowing across this section. The sign of the water flux indicates its direction, and hence provide an Inflow or an outflow of anthropogenic carbon. The total storage is the sum of the net δC_T flux at the strait of Gibraltar and of the δC_T air-sea flux, and is consistent with the sum of all the δC_T store in the Mediterranean Sea.

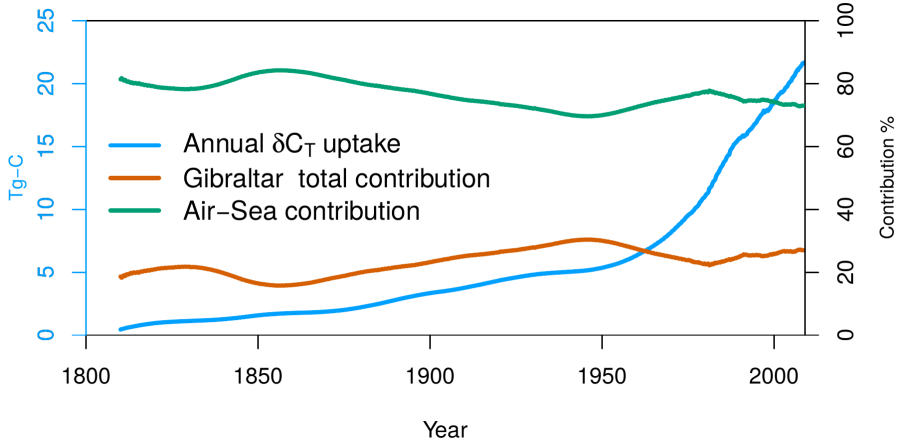

Figure 8. Evolution of the Mediterranean's annual uptake in δC_T (solid, light blue line) , calculated within a 10-year running average to focus on decadal-scale changes Also shown is the percentage of ~~the total δC_T~~ that annual δC_T that entered the Mediterranean Sea ~~from~~ through the ~~air–sea flux of anthropogenic carbon (solid, light blue) and from Strait~~ strait of Gibraltar (solid, ~~purple~~orange line)~~minus that which leaves via the same strait but deeper down (dashed~~, ~~purple). Also shown is~~ and via the ~~Mediterranean Sea's total storage~~ air-sea fluxes (~~dashed~~solid, ~~light blue~~green line).

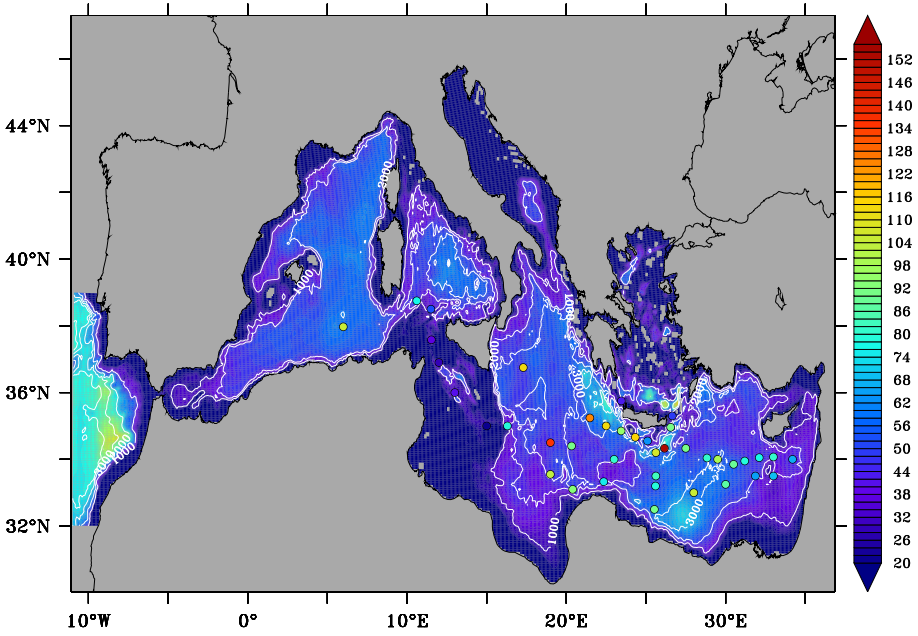

Figure 9. Inventory of δC_{T} (mol m^{-2}) in November 2001 from the MED simulation (color-filled contours) and from Schneider et al. (2010) data-based estimates (color-filled dots). The Mediterranean bathymetry is represented with white isobaths every 1000 m.

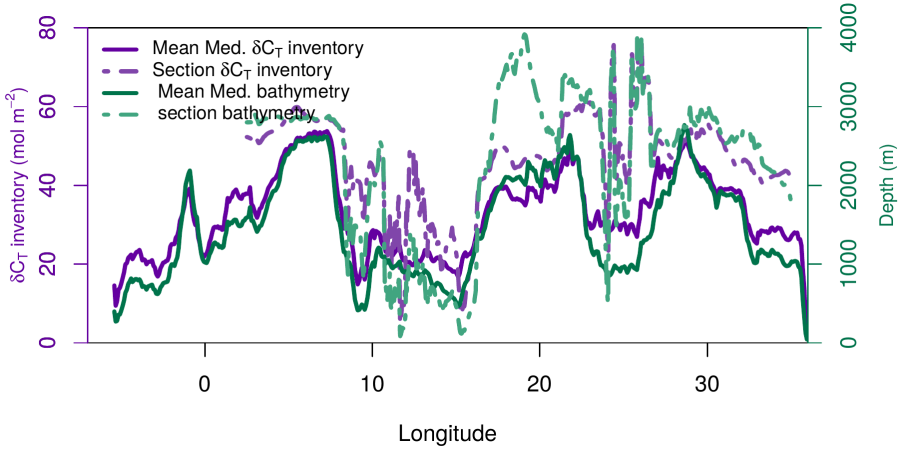

Figure 10. δC_{T} inventory (mol C m^{-2}) along the METEOR M51/2 section (dashed lines) and given as the meridional mean (solid lines) for the MED simulation (~~green~~purple) along with corresponding model bathymetry (~~purple~~green).

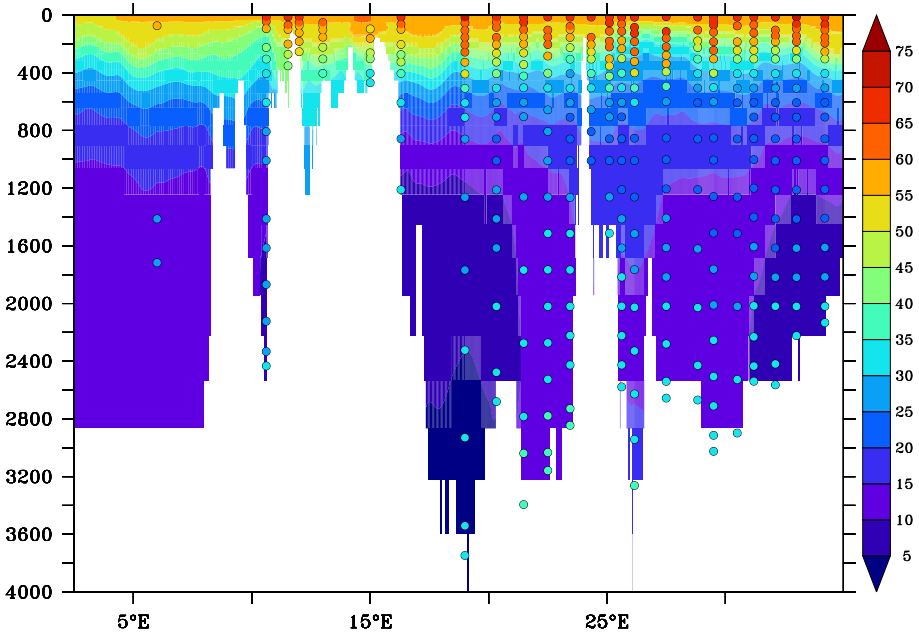

Figure 11. Comparison of δC_{T} ($\mu\mathrm{mol\,kg^{-1}}$) along the METEOR M51/2 section for the model (color-filled contours) and the TTD data-based estimates (color-filled dots) in November 2001.

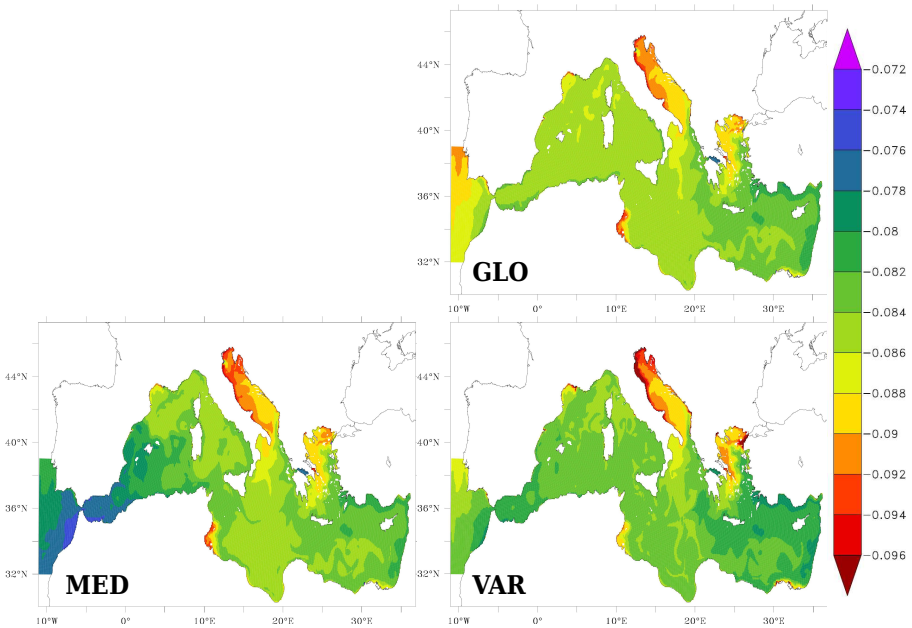

Figure 12. Anthropogenic change in surface pH between 1800 and 2001 for the the GLO (top), MED (bottom left), and VAR (bottom right) simulations.

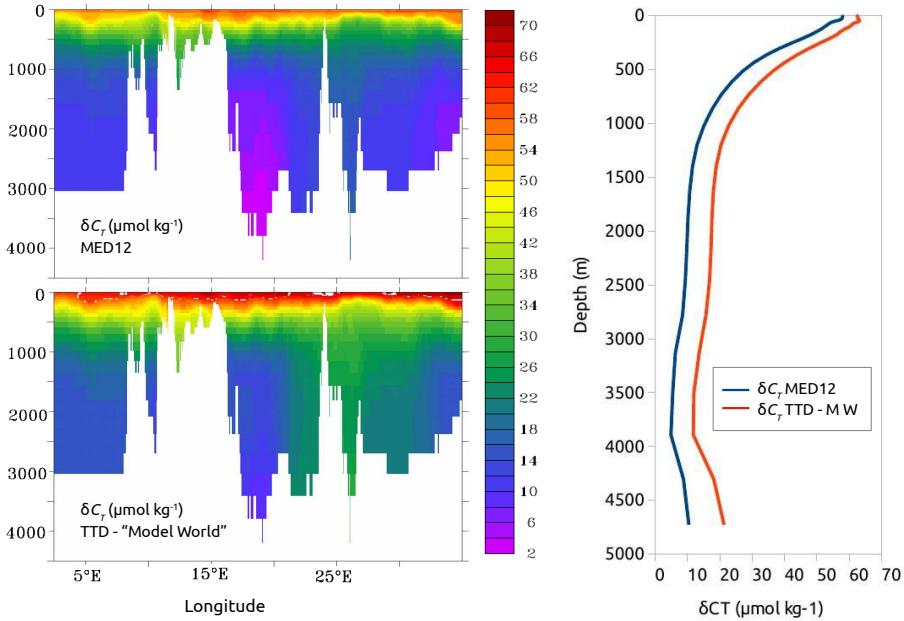

Figure 13. δC_{T} ($\mu\mathrm{mol\,kg^{-1}}$) along the METEOR M51/2 section, estimated with the MED reference simulation (top left) and the TTD method in the model world (bottom left). Also shown are the same results but as area-weighted vertical profiles for the whole Mediterranean Sea (right).

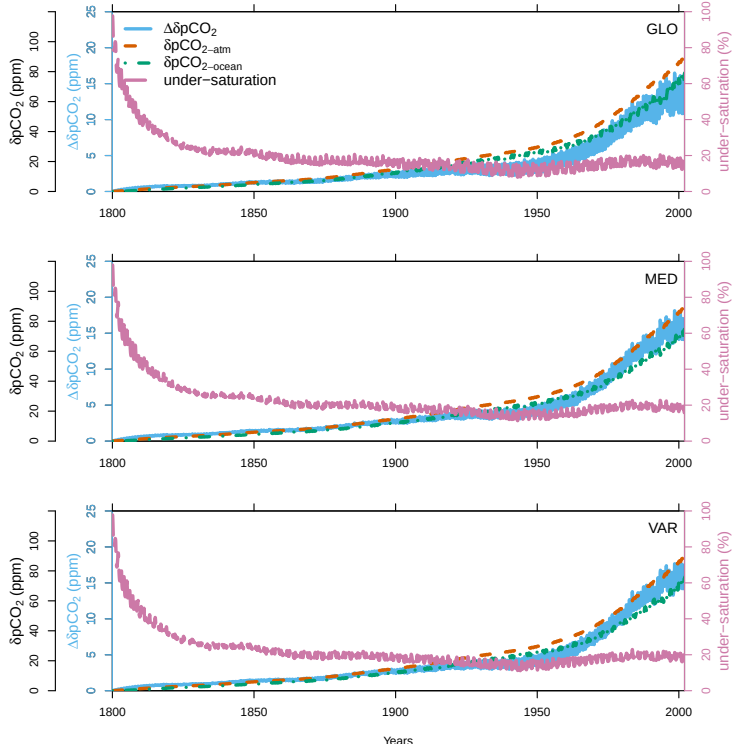

Figure 14. ~~Time~~ Temporal evolution from 1800 to 2001 of ~~C_T~~ spatially averaged δpCO_2 (~~solid~~in ppm) ~~and pH~~ in the atmosphere (dashed ~~) based on simple thermodynamic equilibrium calculations with seacarb (Lavigne and Gattuso, 2011) that vary atmospheric (280 to 450) with 3 different fixed values of total alkalinity: 2300 (purple~~orange), ~~2450~~ the ocean (~~blue~~dashed-dotted green), and ~~2600~~their difference difference $\Delta\delta pCO_2$ (~~light blue~~solid light-blue line). ~~The top panel shows the absolute values, whereas the bottom panel shows~~ Also shown is the ~~change~~ corresponding percent undersaturation of oceanic δpCO_2 (~~anthropogenic perturbation relative to 280~~long dashed purple), defined as $100\left(1-\left(\frac{\delta pCO_{2\,oc}}{\delta pCO_{2\,atm}}\right)\right)$.

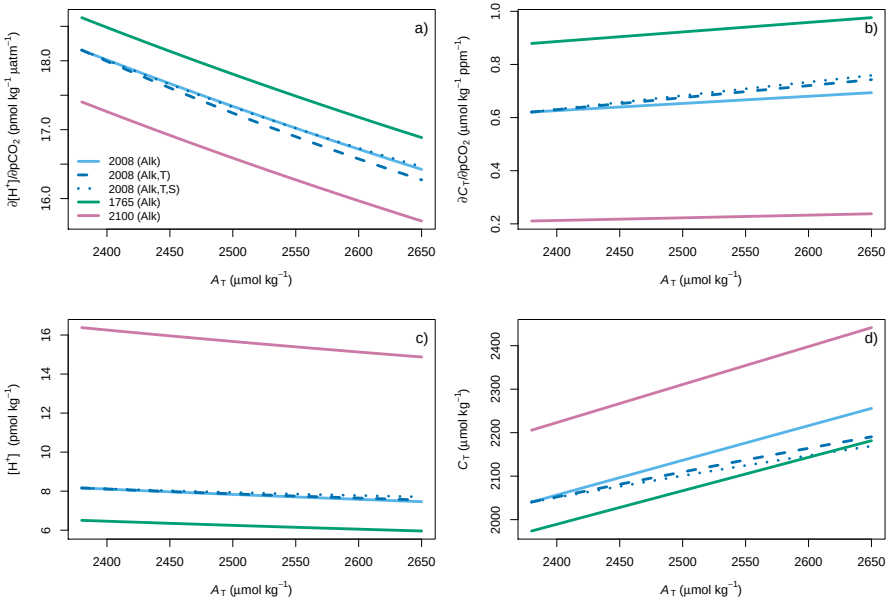

Figure 15. Acidification rate (a - $\partial[H^+]/\partial pCO_2$, in pmol kg^{-1} μatm^{-1}) ; total carbon change rate (b - $\partial C_T/\partial pCO_2$, in μmol kg^{-1} ppm^{-1}); surface H^+ ion concentration (c - in pmol kg^{-1}); and total carbon concentration (d - in μmol kg^{-1}), as a function of alkalinity varied over the observed Mediterranean range (2380 to 2650 μmolkg^{-1}) for 3 different atmospheric pCO_2 levels in 1765 (280 ppm, solid green line), 2008 (385 ppm, solid light-blue line) and 2100 (850 ppm, solid purple line) Also shown are lines for 2008 to illustrate the effects of also varying temperature (dashed blue) and temperature and salinity (dotted blue) over the observed west-to-east range.

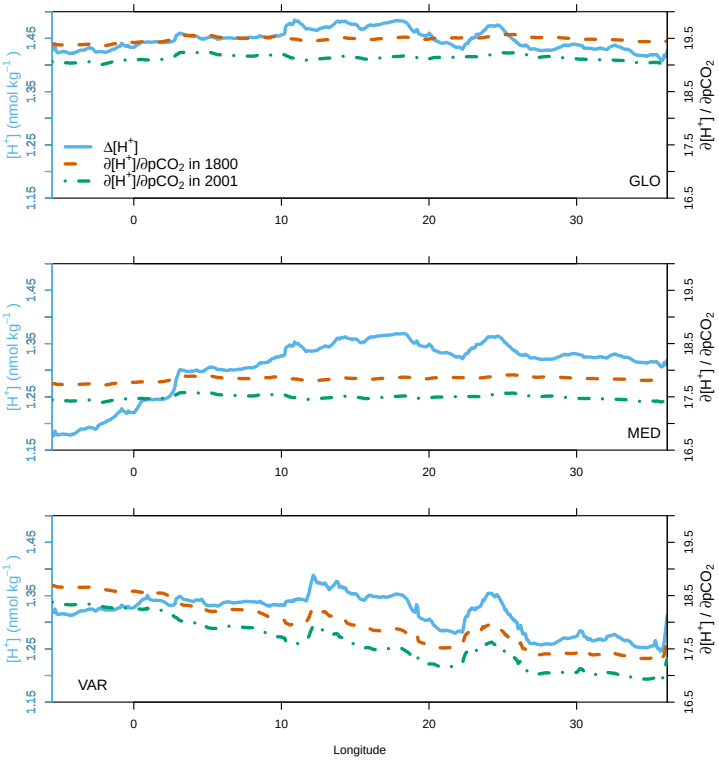

Figure 16. Meridional mean of the acidification rate $\partial[H^+]/\partial pCO_2$ (in pmol kg^{-1} μatm^{-1}) in 1800 (dashed orange) and in 2001 (dashed-dotted green) in the Mediterranean Sea along with the corresponding $[H^+]$ change between 1800 and 2001 in nmol kg^{-1} (solid light-blue). Meridional means are taken from all grid cells with salinities above 32, thus avoiding bias from river mouths.

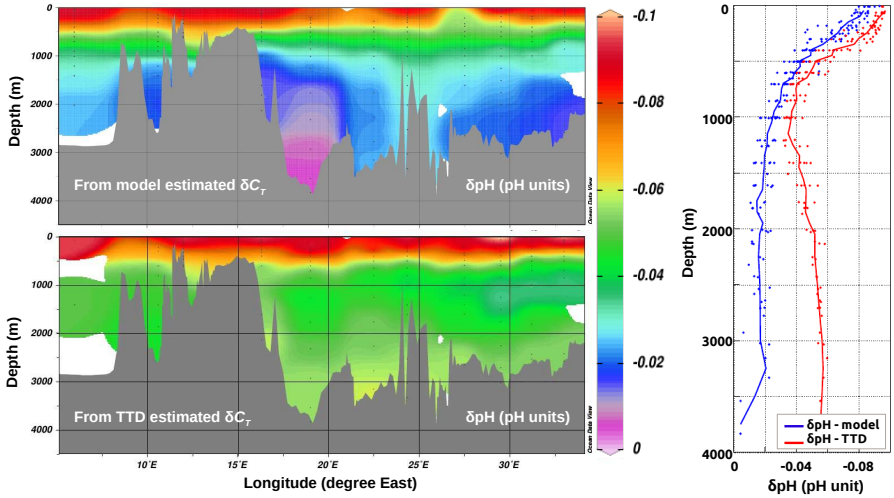

Figure 17. Mediterranean δpH along the METEOR M51/2 section, calculated with δC_{T} from the MED simulation (top left) and from the TTD data-based estimates from Schneider et al. (2010) (bottom left). Also shown are the same results but as mean vertical profiles averaged along the section (right).